Atmos. Chem. Phys. Discuss., doi:10.5194/acp-2016-866, 2016
Manuscript under review for journal Atmos. Chem. Phys.
Published: 10 November 2016

Atmospheric Chemistry and Physics Discussions
Open Access

Title: Biomass burning emissions in north Australia during the early dry season: an overview of the 2014 SAFIRED campaign

Authors:

Marc D. Mallet[1], Maximilien J. Desservettaz[2], Branka Miljevic[1*], Andelija Milic[1], Zoran D. Ristovski[1], Joel Alroe[1], Luke T. Cravigan[1], E. Rohan Jayaratne[1], Clare Paton-Walsh[2], David W.T. Griffith[2], Stephen R. Wilson[2], Graham Kettlewell[2], Marcel V. van der Schoot[3], Paul Selleck[3], Fabienne Reisen[3], Sarah J. Lawson[3], Jason Ward[3], James Harnwell[3], Min Cheng[3], Rob W. Gillett[3], Suzie B. Molloy[3], Dean Howard[4], Peter F. Nelson[4], Anthony L. Morrison[4], Grant C. Edwards[4], Alastair G. Williams[5], Scott D. Chambers[5], Sylvester Werczynski[5], Leah R. Williams[6], V. Holly L. Winton[7,n], Brad Atkinson[8], Xianyu Wang[9], Melita D. Keywood[3*]

Affiliations:

[1]Department of Chemistry, Physics and Mechanical Engineering, Queensland University of Technology, Queensland, Brisbane, 4000, Australia

[2]Centre for Atmospheric Chemistry, University of Wollongong, Wollongong, New South Wales, 2522, Australia

[3]CSIRO Oceans and Atmosphere, Aspendale, Victoria, 3195, Australia

[4]Department of Environmental Sciences, Macquarie University, Sydney, New South Wales, 2109, Australia

[5]Australian Nuclei Science and Technology Organisation, Sydney, New South Wales, 2232, Australia

[6]Aerodyne Research, Inc., Billerica, Massachusetts, 01821, USA

[7]Physics and Astronomy, Curtin University, Perth, Western Australia, 6102, Australia

[8]Bureau of Meteorology, Darwin, Northern Territory, 0810, Australia

[9]National Research Centre for Environmental Toxicology, Brisbane, Queensland, 4108, Australia

[n]Now at the British Antarctic Survey, National Environmental Research Council, Cambridge, CB30HT, UK

Atmos. Chem. Phys. Discuss., doi:10.5194/acp-2016-866, 2016
Manuscript under review for journal Atmos. Chem. Phys.
Published: 10 November 2016

***Corresponding Authors:**

Dr Melita Keywood

Contact Phone: +613 9239 4596

Contact Email: melita.keywood@csiro.au

Dr Branka Miljevic

Contact Phone: +61 7 3138 3827

Contact Email: b.miljevic@qut.edu.au

Keywords:

Biomass burning | savannah fires | greenhouse gases | aerosols | mercury

Atmos. Chem. Phys. Discuss., doi:10.5194/acp-2016-866, 2016
Manuscript under review for journal Atmos. Chem. Phys.
Published: 10 November 2016

Atmospheric Chemistry and Physics Discussions

Abstract

The SAFIRED (Savannah Fires in the Early Dry Season) campaign took place from 29th of May, 2014 until the 30th June, 2014 at the Australian Tropical Atmospheric Research Station (ATARS) in the Northern Territory, Australia. The purpose of this campaign was to investigate emissions from fires in the early dry season in northern Australia. Measurements were made of biomass burning aerosols, volatile organic compounds, polycyclic aromatic carbons, greenhouse gases, radon, mercury cycle, and trace metals. Aspects of the biomass burning aerosol emissions investigated included; emission factors of various emitted species, physical and chemical aerosol properties, aerosol aging, micronutrient supply to the ocean, nucleation, and aerosol water uptake. Over the course of the month-long campaign, biomass burning signals were prevalent and emissions from several large single burning events were observed at ATARS.

Biomass burning emissions dominated the gas and aerosol concentrations in this region. Nine major biomass burning events were identified and associated with intense or close individual smoke plumes. Dry season fires are extremely frequent and widespread across the northern region of Australia, which suggests that the measured aerosol and gaseous emissions at ATARS are likely representative of signals across the entire region of north Australia. Air mass forward trajectories show that these biomass burning emissions are carried north west over the Timor Sea and could influence the atmosphere over Indonesia and the tropical atmosphere over the Indian Ocean.

The outcomes of this campaign will be numerous. This region is an environment with little human impact and provides a unique look into the characteristics of biomass burning aerosol without the influence of other significant emission sources. Relationships between the aerosol physical and chemical properties, gas concentrations

Atmos. Chem. Phys. Discuss., doi:10.5194/acp-2016-866, 2016
Manuscript under review for journal Atmos. Chem. Phys.
Published: 10 November 2016

and meteorological data for the entire month will provide fundamental knowledge required to understand the influence of early dry season burning in this tropical region on the atmosphere. In this paper we present characteristics of the biomass burning observed at the sampling site and provide an overview of the more specific outcomes of the SAFIRED campaign.

Atmos. Chem. Phys. Discuss., doi:10.5194/acp-2016-866, 2016
Manuscript under review for journal Atmos. Chem. Phys.
Published: 10 November 2016

1. Introduction

Tropical north Australia is dominated by savannah ecosystems. This region consists of dense native and exotic grasslands and scattered trees and shrubs. Conditions are hot, humid and wet in the summer months of December through March with hot, dry conditions for the rest of the year giving rise to frequent fires between June and November each year. Human settlements are relatively scarce in northern Australia, outside of the territory capital, Darwin (population of 146 000). To the north of the continent are the tropical waters of the Timor Sea, as well as the highly populated Indonesian archipelago. South of the savannah grasslands are the Tanami, Simpson and Great Sandy Deserts, spanning hundreds of thousands of square kilometers. Emissions from fires in the savannah regions of northern Australia are therefore the most significant regional source of greenhouse and other trace gases, as well as atmospheric aerosol. Globally, savannah and grassland fires are the largest source of carbon emissions (van der Werf et al., 2010;Shi et al., 2015) and play a significant role in the earth's radiative budget. It is therefore important to quantify, characterise and fully understand the emissions from savannah fires in northern Australia, taking into account the complexity, variability and diversity of the species emitted.

In Australia approximately 550 000 km^2 of tropical and arid savannahs burn each year (Meyer et al., 2012;Russell-Smith et al., 2007), representing 7% of the continent's land area. In the tropical north of Australia, the fires during the early dry season in May/June consist of naturally occurring and accidental fires, as well as prescribed burns under strategic fire management practice to reduce the frequency and intensity of more extensive fires in the late dry season in October and November (Andersen et al., 2005). These fires in the early dry season burn with a low to moderate intensity and are

Atmos. Chem. Phys. Discuss., doi:10.5194/acp-2016-866, 2016
Manuscript under review for journal Atmos. Chem. Phys.
Published: 10 November 2016

normally confined to the grass-layer. Events where fires reach the canopy level are rare. These prescribed burns are an important process for the region and are undertaken by local landholders with permits, as well as government supported bodies and volunteers. There has been a recent push to reinstate traditional Aboriginal fire management regimes in this region (Russell-Smith et al., 2013). Other fire management regimes are implemented in similar environments around the world, such as the savannah ecosystems of Africa (Govender et al., 2006) or the chaparral grasses in the United States (Akagi et al., 2012). In general, fire management regimes are considered to benefit regional biodiversity and can lead to the long-term increase in living biomass, resulting in a reduction of greenhouse gas emissions (Russell-Smith et al., 2013). Quantifying the emissions from dry season fires on regional scales is essential for understanding the impact of these fires on the local and global atmosphere.

The components and concentrations of emissions from savannah fires are dependent upon the vegetation and burning conditions. While CO_2 is the primary product of biomass burning (BB), incomplete combustion also results in the emission of many other trace gases such as CO, CH_4, NOx, N_2O as well as non methane organic compounds (NMOCs) and aerosol particles composed of elemental carbon, organic carbon and some inorganic material (Crutzen and Andreae, 1990). The state of organics in biomass burning aerosols can vary significantly due to the type of plant material burned, the characteristics of the fires themselves as well as through aging processes in the atmosphere.

The effects of these emissions on radiative forcing are complex. The global average radiative forcing due to biomass burning aerosol-radiation interaction is estimated in

Atmos. Chem. Phys. Discuss., doi:10.5194/acp-2016-866, 2016
Manuscript under review for journal Atmos. Chem. Phys.
Published: 10 November 2016

the 5th International Panel on Climate Change report as 0.0 W m^{-2} with an uncertainty range of -0.20 to +0.20 Wm^{-2} (Bindoff et al., 2013). It is well known that greenhouse gases have a positive radiative forcing, heating up the atmosphere. Light absorbing carbon in the aerosol phase will also result in a positive radiative forcing (Jacobson, 2001) by absorbing shortwave radiation. Conversely, the presence of aerosol organic and inorganic matter can result in a negative radiative forcing by scattering solar radiation (Penner et al., 1998). In addition, biomass burning has been shown to be a significant source of cloud condensation nuclei (CCN), despite typically being composed of weakly hygroscopic substances (Lawson et al., 2015), due to the high number of particles emitted. This can result in a change in cloud droplet concentrations and volume, thereby influencing cloud formation, albedo and lifetime. The contribution of each species to the overall radiative forcing is also likely to change as smoke plumes age (Liousse et al., 1995). Furthermore, not all biomass burning aerosol will interact with radiation in the same way. For example, fresh BB emissions in the tropics has been observed to be more absorbing than those from boreal forest fires(Wong and Li, 2002). The role of biomass burning emissions is not limited to the Earth's radiative budget. Certain species of emissions (e.g., mercury) can be deposited and sequestered in soil (Gustin et al., 2008), vegetation (Rea et al., 2002) or bodies of water (LaRoche and Breitbarth, 2005).

There is a need for a better scientific understanding of the influence biomass burning has on atmospheric composition and air quality (Kaiser and Keywood, 2015). Furthermore, the tropics are disproportionately under-sampled and the atmospheric and ocean processes in these regions are of both regional and global consequence. The

Atmos. Chem. Phys. Discuss., doi:10.5194/acp-2016-866, 2016
Manuscript under review for journal Atmos. Chem. Phys.
Published: 10 November 2016

SAFIRED campaign will contribute towards better understanding biomass burning emissions and the atmospheric composition in tropical Australia.

2. Description of experiment

2.1 Site

The Australian Tropical Atmospheric Research Station (ATARS; 12°14'56.6"S, 131°02'40.8"E) is located on the Gunn Point peninsula in northern Australia (see Figure 1). ATARS is operated by the Australian Bureau of Meteorology and the CSIRO (Commonwealth Scientific and Industrial Research Organisation). Standard meteorological measurements (wind velocity, atmospheric pressure, precipitation) run permanently at ATARS and two laboratories are in place for the installation of other instruments. The SAFIRED campaign took place from 29th May 2014 until the 30th June 2014, with personnel and instruments from nine institutes utilising these laboratories to make comprehensive gaseous and aerosol measurements during this period of the early dry season.

2.2 Instruments and measurements

2.2.1 Trace Gases

Greenhouse gases

Continuous measurement of CO_2, CO, CH_4 and N_2O were made using a high precision FTIR trace gas and isotope Spectronus analyser, developed by the Centre for Atmospheric Chemistry at the University of Wollongong. The analyser combines a Fourier Transform Infrared (FTIR) Spectrometer (Bruker IRcube), a pressure and

Atmos. Chem. Phys. Discuss., doi:10.5194/acp-2016-866, 2016
Manuscript under review for journal Atmos. Chem. Phys.
Published: 10 November 2016

temperature controlled multi-pass cell and an electronically cooled mercury cadmium telluride detector. A detailed description of the instrument and concentration retrieval technique are available in Griffith et al. (2012) and Griffith (1996).

Ozone and other trace gases

A Multi Axis Differential Optical Absorption Spectrometer (MAX-DOAS) was installed on the top of one of the laboratories during the campaign. The technique has been shown to provide vertical profile of nitrogen dioxide, ozone, sulfur dioxide, formaldehyde, glyoxal and aerosol extinction (Sinreich et al., 2005;Honninger et al., 2004). The MAX-DOAS instrument used in this campaign was designed and built at the University of Wollongong. It consists of a vertically rotating prism capturing scattered solar radiation at different angles (1°, 2°, 4°, 8°, 16°, 30° and a reference at 90°) into a fibre optic that carries the radiation to a UV-Visible spectrometer (AvaSpec – ULS3648). Furthermore, a Thermo Scientific model 49i UV Photomeric Ozone analyser was used to measure ozone concentrations.

Non methane organic compounds

Online NMOC measurements were made using a high sensitivity Proton Transfer Reaction-Mass Spectrometer (PTR-MS; Ionicon Analytik) using H_3O^+ as the primary ion. The inlet was 10 m in length and drew air at 5 L min^{-1} from 2 m above the roof (approx 5.5 m above ground level). The PTR-MS ran with inlet and drift tube temperature of 60 ºC, 600 V drift tube, and 2.2 mbar drift tube pressure, which equates to an energy field of 135 Td. The PTR-MS sequentially scanned masses 15-190, with 1 second dwell time. The PTR-MS operated with the aid of auxiliary equipment which regulates the flow of air in the sample inlet and controls whether the PTR-MS is sampling ambient or zero air or calibration gas (Galbally et al., 2007). During the

Atmos. Chem. Phys. Discuss., doi:10.5194/acp-2016-866, 2016
Manuscript under review for journal Atmos. Chem. Phys.
Published: 10 November 2016

Atmospheric Chemistry and Physics Discussions

campaign the PTR-MS was calibrated once per day for the following compounds using certified gas standards from Apel Riemer Environmental Inc, USA and Air Liquide Specialty Gases, USA: acetaldehyde, acetone, acetonitrile, benzene, methacrolein, methanol, methyl ethyl ketone, toluene, 1,3,5-trimethyl benzene, m-xylene, chlorobenzene, alpha pinene, 1,2-dichlorobenzene, 1,3,4 trichlorobenzene, dimethyl sulphide and isoprene. Calibration data were used to construct sensitivity plots, which were used to calculate approximate response factors for other masses not specifically calibrated.

During sampling, carbonyls and dicarbonyls were trapped on S10 Supelco cartridges, containing high-purity silica adsorbent coated with 2,4-dinitrophenylhydrazine (DNPH, where they were converted to the hydrazone derivatives. Samples were refrigerated immediately after sampling until analysis. The derivatives were extracted from the cartridge in 2.5 mL of acetonitrile and analysed by high performance liquid chromatography with diode array detection. The diode array detection enables the absorption spectra of each peak to be determined. The difference in the spectra highlights which peaks in the chromatograms are mono- or dicarbonyl DNPH derivatives and, along with retention times, allows the identification of the dicarbonyls glyoxal and methylglyoxal. Further details can be found in Lawson et al. (2015).

PAHs

PAHs were sampled through a high-volume air sampler (Kimoto Electric Co., LTD.) using a sampling rate typically at ~60 m^{-3} h^{-1}. The sampling rate was calibrated using an orifice plate prior to the sampling campaign and the sampling volume was calculated based on the calibrated sampling rate and sampling duration. A bypass gas meter installed on the sampler was used to monitor any anomalous fluctuation of the sampling

Atmos. Chem. Phys. Discuss., doi:10.5194/acp-2016-866, 2016
Manuscript under review for journal Atmos. Chem. Phys.
Published: 10 November 2016

Atmospheric Chemistry and Physics Discussions

rate during the sampling period. Particle-associated and gaseous PAHs were collected on glass fibre filters (Whatman™, 203×254 mm, grade GF/A in sheets) and subsequent polyurethane foam plugs respectively. The glass fibre filters and polyurethane foam, along with the field blank samples, were extracted separately using an Accelerated Solvent Extractor (Thermo Scientific™ Dionex™ ASE™ 350) after being spiked with a solution containing 7 deuterated PAHs (i.e. $^{2}D_{10}$-phenanthrene, $^{2}D_{10}$-fluoranthene, $^{2}D_{12}$-chrysene, $^{2}D_{12}$-benzo[b]fluoranthene, $^{2}D_{12}$-BaP, $^{2}D_{12}$-indeno[1,2,3-cd]pyrene, $^{2}D_{12}$-benzo[g,h,i]perylene) at different levels as internal standards for quantification purposes. Concentrated extracts were cleaned up by neutral alumina and neutral silica. Eluents were carefully evaporated to near dryness and refilled with 250 pg of $^{13}C_{12}$-PCB (polychlorinated biphenyl) 141 (in 25 µL isooctane) employed as the recovery/instrument standard for estimating the recoveries of the spiked internal standards and monitoring the performance of the analytical instrument. Samples were analysed using a Thermo Scientific™ TRACE™ 1310 gas chromatograph coupled to a Thermo Scientific™ double-focusing system™ Magnetic Sector high resolution mass spectrometer. The HRMS was operated in electron impact-multiple ion detection mode and resolution was set to ≥ 10,000 (10% valley definition). An isotopic dilution method was used to quantify 13 PAH analytes including phenanthrene, anthracene, fluoranthene, pyrene, benzo[a]anthrancene, chrysene, benzo[b]fluoranthene, benzo[k]fluoranthene, benzo[e]pyrene, BaP, indeno[1,2,3-cd]pyrene, dibenzo[a,h]anthracene, benzo[g,h,i]perylene.

Mercury

Total gaseous mercury, gaseous elemental mercury + gaseous oxidised mercury (TGM; GEM + GOM), was sampled from a 10 m mast and measured via gold pre-concentration and cold vapour atomic fluorescence spectroscopy using a Tekran 2537X instrument.

Atmos. Chem. Phys. Discuss., doi:10.5194/acp-2016-866, 2016
Manuscript under review for journal Atmos. Chem. Phys.
Published: 10 November 2016

Simultaneously, GEM, GOM and PBM were individually measured using a Tekran 2537B connected to a combined Tekran 1130/1135 speciation unit sampling at a 5.4 m height. The sampling train of the 1130/1135 collects first GOM (KCl-coated denuder) then PBM (quartz wool pyrolyser) in series from a 10 L min^{-1} sampling flow, allowing GEM only to flow onwards for detection by subsampling by the 2537B. Due to the small atmospheric concentrations of GOM and PBM, pre-concentration occurred over a 1-hour period with subsequent analysis taking an additional hour. Continuous measurements of GEM at 5-minute resolution were made possible for the 2537B unit by rotating pre-concentration/analysis roles of the two internal gold traps. Both 2537 units sampled at 1 L min^{-1} and were calibrated every 23 hours using an internal mercury permeation source. For more information on the 2537 and 1130/1135 systems see Landis et al. (2002) and Steffen et al. (2008).

GEM fluxes were measured using the methods outlined in Edwards et al. (2005). Air samples were drawn at heights of 5.2 and 8.0 m through 46.4 m of nylon tubing using a PTFE diaphragm pump operating at 10 L min^{-1}. Subsampling from this flow through a 0.2 µm PTFE filter at 1 L min^{-1} by a Tekran 2537A, and switching between sample intakes, allowed resolution of a GEM gradient every 30 minutes. The transfer velocity was measured using a Campbell Scientific CSAT3 sonic anemometer and LI-COR 7200 closed path infrared gas analyser for CO_2, both located on the same tower as the gradient intakes at 6.6 m and sampling at 20 Hz.

Radon

Radon-222 (radon) is a naturally occurring radioactive noble gas that arises from the alpha-particle decay of radium-226, which is ubiquitous in most soil and rock types. With a half-life of 3.82 days, radon has thus proven to be an excellent indicator of recent

Atmos. Chem. Phys. Discuss., doi:10.5194/acp-2016-866, 2016
Manuscript under review for journal Atmos. Chem. Phys.
Published: 10 November 2016

(within 2-3 weeks) terrestrial influences on air masses for observations at coastal or island sites (Chambers et al., 2014). Radon is unreactive and poorly soluble, and its only atmospheric sink is radioactive decay. Furthermore, it has a half-life comparable to the lifetimes of short-lived atmospheric pollutants (e.g., NOx, SO_2) and atmospheric residence time of water and aerosols. Radon's unique combination of physical characteristics make it an ideal tracer for (i) regional air mass transport studies, in which it is often used in conjunction with air mass back trajectories for fetch analyses (Williams et al., 2009;Chambers et al., 2014); (ii) investigations of vertical mixing processes within the daytime convective boundary layer (Williams et al., 2011) or nocturnal boundary layer (Chambers et al., 2015); (iii) identifying periods of minimal terrestrial influence on a measured air mass ("baseline" studies; (Chambers et al., 2016)); (iv) performing regional flux or inventory analyses for trace atmospheric species with similar source distributions (Biraud et al., 2000) and (v) evaluating the performance of transport and mixing schemes in climate and chemical-transport models (Locatelli et al., 2015).

In order to measure Radon concentrations, a 700 L dual-flow-loop two-filter radon detector, designed and built by the Australian Nuclear Science and Technology Organisation (Whittlestone and Zahorowski, 1998;Chambers et al., 2014), was installed at the ATARS in 2011 and has been fully operational since July 2012. The detector provided continuous hourly radon concentrations for the duration of the SAFIRED campaign, sampling air at 40 L min^{-1} from 12 m above ground level through 25 mm high-density polyethylene agricultural pipe. A coarse aerosol filter and dehumidifier were installed "upstream" of the detector, as well as a 400 L delay volume to ensure that thoron (^{220}Rn, half-life 55 s) concentrations in the inlet air stream were reduced to

Atmos. Chem. Phys. Discuss., doi:10.5194/acp-2016-866, 2016
Manuscript under review for journal Atmos. Chem. Phys.
Published: 10 November 2016

less than 0.5 % of their ambient values. The detector's response time is around 45 minutes, and the lower limit of detection is 40 - 50 mBq m^{-3}. Calibrations are performed on a monthly basis by injecting radon from a PYLON 101.15±4% kBq Ra-226 source (12.745 Bq min^{-1} ^{222}Rn), traceable to NIST standards, and instrumental background is checked every 3 months. In post processing, half-hourly raw counts were integrated to hourly values before calibration to activity concentrations (Bq m^{-3}).

Aerosols

Aerosol Drying System

An Automated Regenerating Aerosol Diffusion Dryer (ARADD) is permanently installed on the roof of the laboratory containing the aerosol instrumentation for this campaign. This was used in front of the aerosol manifold to continuously dry the aerosol sample. The ARADD design, similar to that described by Tuch et al. (2009), continuously conditions the aerosol sample to a relative humidity of below 40% with maximum aerosol transmission efficiency. The ARADD utilizes two diffusion drying columns in parallel, each containing 7 stainless steel mesh tubes of 10 mm internal diameter and approximately 800 mm length, surrounded by a cavity packed with silica gel. The aerosol sampled is directed into one column at a time, while the other column is regenerated by an ultra-dry compressed air system. All flows are controlled by software that directs sample flow and compressed air flow to the appropriate column with a series of valves. The ARADD has a Total Suspended Particulate style intake at the inlet of the aerosol sample path, and a sample manifold at the exit of the system to provide sampling take-offs for the various aerosol instruments connected to the ARADD. Flow through the ARADD is provided by the instruments and pumps connected downstream. The ambient and inlet relative humidity for the entire sampling period were logged and are displayed in Supplementary Figure 1.

Atmos. Chem. Phys. Discuss., doi:10.5194/acp-2016-866, 2016
Manuscript under review for journal Atmos. Chem. Phys.
Published: 10 November 2016

Atmospheric Chemistry and Physics Discussions

Aerosol Size

Aerosol size distributions were measured with a Scanning Mobility Particle Sizer (SMPS). A TSI 3071 long-column electrostatic classifier with a TSI 3772 Condensation Particle Counter (CPC) measured the size distribution over a range of 14 nm to 670 nm at a scan interval of 5 minutes.

In addition to the aerosol size distributions measured by the SMPS, neutral and charged aerosol particle distributions from 0.8 nm to 42 nm were measured using a Neutral cluster and Air Ion Spectrometer (NAIS)(Manninen et al., 2009;Mirme et al., 2007). In this study, the NAIS was set to operate in a cycle of 4 min including ion and neutral particle sampling periods of 2 and 1 minute, respectively, with the remaining minute being an offset period which is required to neutralize and relax the electrodes. The total sampling air flow was 60 L min^{-1}, the high flow rate being used to minimize ion diffusion losses and maximize the measured ion concentration sensitivity. Ion losses are accounted for during post-processing of the data by the software (Mirme et al., 2007).

Aerosol Composition and Water Uptake

PM_1 and PM_{10} 12-hour filter samples (night and day) were collected on a TAPI 602 Beta plus particle measurement system (BAM). Portions of the PM_1 filters have been analysed for elemental and organic carbon mass loadings using a DRI Model 2001A Thermal-Optical Carbon Analyzer following the IMPROVE-A temperature protocol (Chow et al., 2007b). Additional portions of the PM_1 filters were extracted in 5 ml of 18.2 mΩ de-ionized water and preserved using 1% chloroform. These extracts will be analysed for major water-soluble ions by suppressed ion chromatography and for

Atmos. Chem. Phys. Discuss., doi:10.5194/acp-2016-866, 2016
Manuscript under review for journal Atmos. Chem. Phys.
Published: 10 November 2016

anhydrous sugars including levoglucosan by high-performance anion-exchange chromatography with pulsed amperometric detection (Iinuma et al., 2009).

Daily aerosol filters were collected using two Ecotech 3000 high-volume volumetric flow controlled aerosol samplers with PM_{10} size selective inlets. One high-volume sampler was used to collect aerosols on acid cleaned Whatman 41 filters to determine the soluble and total fraction of trace metals. Soluble trace metals were extracted from a filter aliquot using ultra-pure water (>18.2 mΩ) leaching experiments. Total trace metal concentrations were determined by digesting a second filter aliquot with concentrated nitric and hydrofluoric acids. Leachates and digested solutions were analysed by high resolution inductively couple plasma mass spectrometry. The second sampler was used to collect a set of aerosol samples on quartz filters for elemental and organic carbon analysis following (Chow et al., 2007a), and major anion and cation analysis.

The volatility and hygroscopicity of 50 nm and 150 nm particles were measured with a custom built Volatility and Hygroscopicity Tandem Differential Mobility Analyser (VH-TDMA). Inlet dried particles were size selected (alternating between 50 and 150 nm) using a TSI 3080 electrostatic classifier. Scans alternated between two different sample pathways. In the first, after size selection, particles were passed through a thermodenuder set to 120°C. The sample line was then split so that half went to an SMPS comprised of a TSI 3080 classifier and a TSI 3010 CPC (V-TDMA). The rest of the sample was passed through a humidifying system that exposed the particles to a relative humidity of 90% before being brought into another SMPS with a 3080 classifier and 3010 CPC (H-TDMA). Alternatively, the thermodenuder was bypassed in every

Atmos. Chem. Phys. Discuss., doi:10.5194/acp-2016-866, 2016
Manuscript under review for journal Atmos. Chem. Phys.
Published: 10 November 2016

second scan so that the V-TDMA was used to verify the size selection and the H-TDMA was able to observe the hygroscopic growth of ambient particles. Each scan ran for 3 minutes, giving a full set of data every 12 minutes.

The chemical composition and properties of non-refractory sub-micron particles were investigated with a compact Time-of-Flight Aerosol Mass Spectrometer (cToF-AMS, Aerodyne Research, Inc.) and a Time of Flight Aerosol Chemical Speciation Monitor (ToF-ACSM, Aerodyne Research, Inc.). Both of these instruments operate with the same principle and have many identical components. An aerodynamic lens in the inlet of each instrument focuses the particles into a beam and differential pumping removes most of the gas phase. Particles are flash vaporized at 600°C and ionized by electron impact before passing through a time-of-flight mass spectrometer to a multi-channel plate detector in the cToF-AMS and a dynode detector in the ToF-ACSM. The cToF-AMS has the added benefit of having a particle Time-of-Flight (pToF) mode, which allows the size resolved chemical composition to be measured. Both instruments sampled through a $PM_{2.5}$ inlet and nafion dryer. In addition, the inlet of the cToF-AMS was incorporated into the VH-TDMA system, so that when the VH-TDMA was measuring ambient particles, the cToF-AMS would draw particles through the thermodenuder set at 120°C and vice-versa. This gives additional information about the chemical composition of the volatile component of submicron particles.

The number of particles activated to cloud droplets were measured using a Continuous-Flow Steam Wise Thermal Gradient Cloud Condensation Nuclei Counter (CCNC) from Droplet Measurement Technologies Inc. (DMT, model No. 100). Particles were

Atmos. Chem. Phys. Discuss., doi:10.5194/acp-2016-866, 2016
Manuscript under review for journal Atmos. Chem. Phys.
Published: 10 November 2016

exposed to a 0.5% supersaturation and activated particles greater than 1μm were counted with an Optical Particle Counter using a 50 mW, 658 nm laser diode.

Back trajectories

Hourly 10-day air mass back trajectories terminating at ATARS were produced using the NOAA HYSPLIT model (Draxler and Rolph, 2003), and catalogued in a data base for use with the SAFIRED campaign data set. Global Data Assimilation System input files with 0.5° resolution were obtained from NOAA ARL FTP site (http://ready.arl.noaa.gov/gdas1.php) to drive the HYSPLIT model.

Satellite detection of fires

Data on the location of fires was collected from the Australian national bushfire monitoring system, Sentinel Hotspots. Hotspot locations are derived from the Moderate Resolution Imaging Spectroradiometer (MODIS) sensors on the Terra and Aqua satellites and the Visible Infrared Imaging Radiometer Suite (VIIRS) sensor on the Suomi NPP satellite. The Terra, Aqua and Suomi NPP satellites fly over the region around ATARS at approximately 10:30 am, 3 pm and 2:30 pm, respectively. Detection of fires is therefore limited to those that are flaming during these times.

Atmos. Chem. Phys. Discuss., doi:10.5194/acp-2016-866, 2016
Manuscript under review for journal Atmos. Chem. Phys.
Published: 10 November 2016

Atmospheric Chemistry and Physics Discussions

3. Overview of Campaign

Fires and air masses

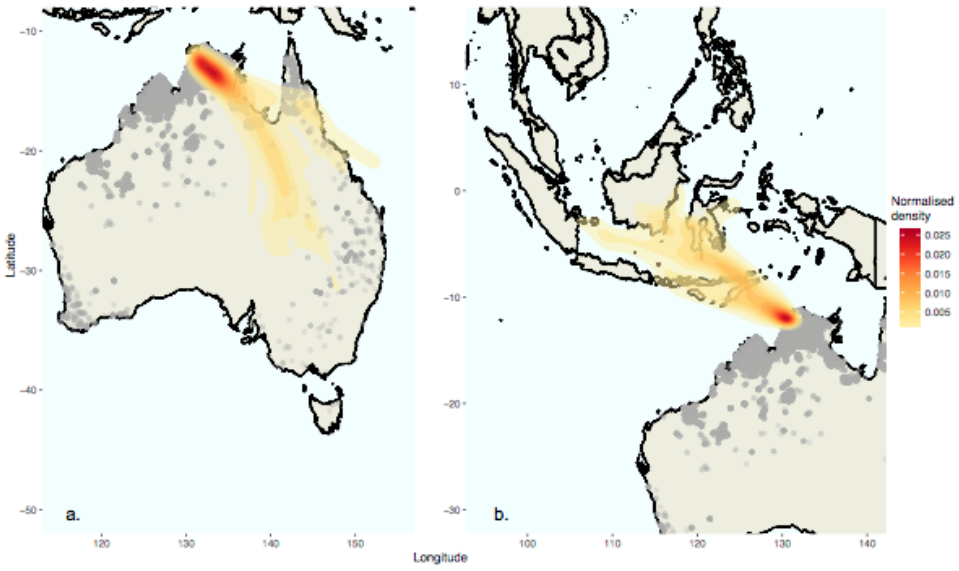

Figure 1 The HYSPLIT (a) back and (b) forward trajectories to and from the ATARS site, truncated to five days. The colour scale represents the air mass trajectory density, normalised to 1. Grey dots are MODIS and VIIRS detected hotspots from the 30th of May 2016 until the 29th of June 2016.

Thousands of fires were observed in during the period of the SAFIRED campaign in Australia by the MODIS and VIIRS sensors on the Terra and Aqua NASA satellites. The vast majority of these occurred in the savannah regions of northern Australia (Figure 1). The number of detected fires on each day within 10 km, 20 km, 50 km, 100 km and 200 km of the sampling location was determined (Figure 2). Several fires within 10km were detected on the 30th of May and the 9th, 10th, 25th and the 26th of June. These correspond with the highest gaseous and aerosol signals. The periods between the 11th and 24th of June had very few detected fires within 50km of the station. Satellite flyby times were in the early afternoon local time each day and therefore fires not occuring during these times would not be recorded. Airmass back trajectories from the ATARS

Atmos. Chem. Phys. Discuss., doi:10.5194/acp-2016-866, 2016
Manuscript under review for journal Atmos. Chem. Phys.
Published: 10 November 2016

site show that air masses over the study period were predominately southeasterly (Figures 1a and 4c), generally over the regions where fires were frequently detected.

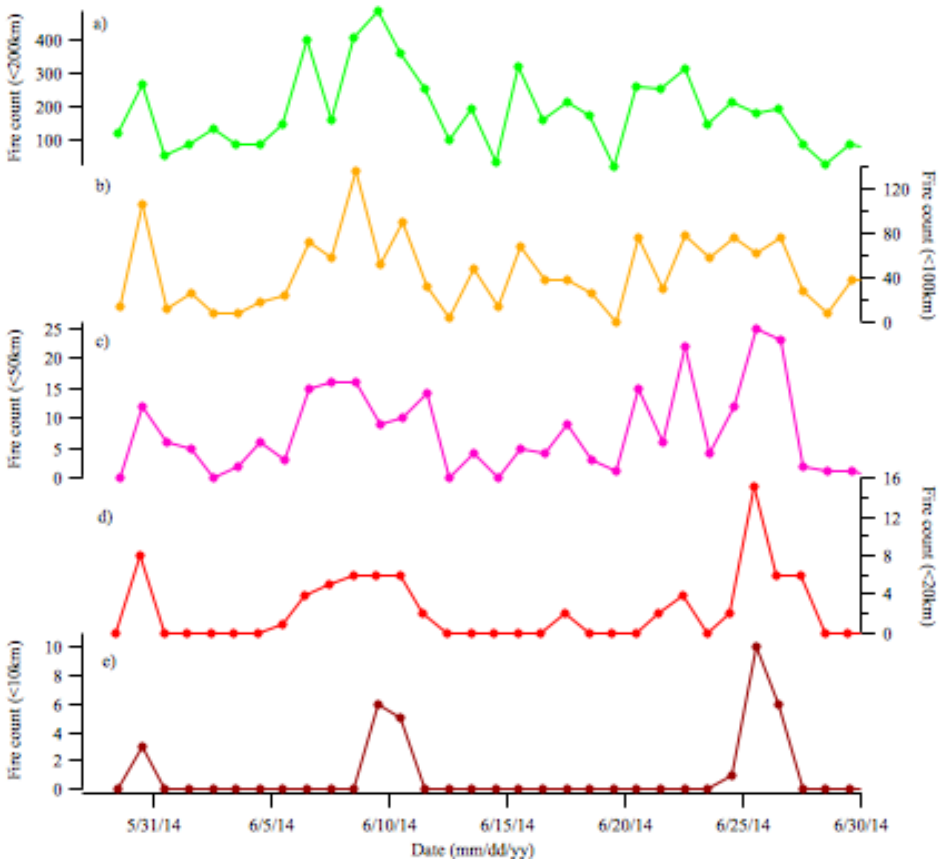

Figure 2 The number of hotspots observed each day within (a) 200 km, (b) 100 km, (c) 50 km, (d) 20 km and (e) 10 km of the ATARS, as detected by the MODIS and VIIRS sensors on the Terra and Aqua satellites.

Afternoon radon concentrations provide further information regarding the regional air mass fetch and the degree of contact with the land surface (red line, Figure 3a). Over the campaign period, air masses with the least terrestrial fetch (low radon indicates strongest oceanic signature) were observed on June 4-6 and 20-22, whereas June 8-9, 17-18 and 29-30 represented periods of particularly extensive continental fetch.

Atmos. Chem. Phys. Discuss., doi:10.5194/acp-2016-866, 2016
Manuscript under review for journal Atmos. Chem. Phys.
Published: 10 November 2016

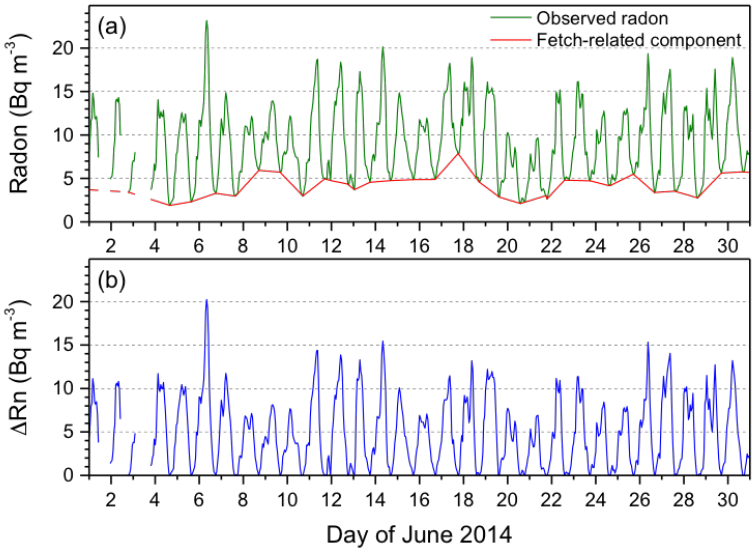

Figure 3 Hourly ATARS radon observations for June 2014: (a) observed hourly data, and afternoon-to-afternoon interpolated values (indicative of changes in the regional air mass fetch); and (b) difference in radon concentration between the hourly observations and interpolated afternoon values (indicative of diurnal variability).

A pronounced diurnal variability can clearly be seen in the ΔRn signal (Figure 3b). Mean hourly diurnal composites of radon concentrations, wind speed, wind direction and dew point temperature at the ATARS site during the period of the SAFIRED campaign are shown in Figure 4. Following the technique described in Chambers et al. (2016), these composites have been computed separately for three diurnal mixing categories based on the mean ΔRn over the 12 hour period 2000-0800 h:

Strong mixing: $\Delta Rn_{12} < 5400$ mBq m^{-3}

Moderate mixing: $5400 \leq \Delta Rn_{12} < 6700$ mBq m^{-3}

Weak mixing: $\Delta Rn_{12} \geq 6700$ mBq m^{-3}

The air masses predominantly originated from the southeast as indicated in Figure 1 and Figure 4c. Starting from approximately 10:00 am each morning, however, sea breeze circulations slowly turn the measured wind direction around from southeast to northeast, before reverting back to the dominant wind direction again at around

Atmos. Chem. Phys. Discuss., doi:10.5194/acp-2016-866, 2016
Manuscript under review for journal Atmos. Chem. Phys.
Published: 10 November 2016

midnight. Wind speeds reached a maximum just before midday and were at their lowest just before midnight (Figure 4b). The "strong mixing" category was associated with generally higher wind speeds, which cause increased mechanical turbulence leading to deeper nocturnal mixing layers (i.e., hinder the development of a shallow nocturnal inversion layer).

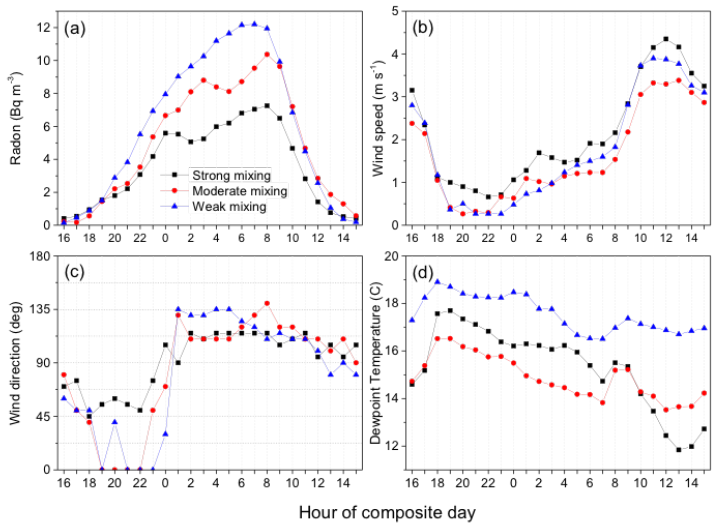

Figure 4 Mean hourly diurnal composite (a) radon, (b) wind speed, (c) wind direction, and (d) dew point temperature at ATARS, as a function of radon-based nocturnal mixing categories.

Gas and Aerosol measurements

The campaign average, standard deviation, median and Q25/Q75 values for the major gaseous and aerosol species are shown in Table 1. The median values for each species are likely to be representative of background concentrations in this region. The average concentrations for most species were higher than the median concentrations, due to the periods of close or intense fires. The extent of the influence of these close fires are demonstrated by the maximum concentrations.

Atmos. Chem. Phys. Discuss., doi:10.5194/acp-2016-866, 2016
Manuscript under review for journal Atmos. Chem. Phys.
Published: 10 November 2016

Atmospheric Chemistry and Physics Discussions

Table 1 The campaign average, standard deviation, maximum, median, Q25 and Q75 values for key measured gas and aerosol species. All parts-per notation refer to mole fractions unless otherwise indicated.

Species (unit)	Average	Standard deviation	Maximum	Median	Q25	Q75
CO (ppb)	229	494	18900	130	87	214
CO_2 (ppm)	404.68	11.539	513.578	402.454	394.728	411.299
O_3 (ppbv)	24.616	9.903	99.784	22.771	17.896	29.778
CH_4 (ppb)	1839.88	68.06	3766.81	1820.11	1802.26	1852.97
N_2O (ppb)	326.329	0.449	334.871	326.276	326.121	326.444
GEM (ng m^{-3})	0.992	0.081	1.734	0.986	0.952	1.020
Acetonitrile (ppb)	0.351	0.629	9.775	0.197	0.129	0.337
Organics (ug m^{-3})	11.081	22.385	347.657	4.160	2.335	13.279
SO_4^{2-} (ug m^{-3})	0.514	0.318	2.254	0.411	0.294	0.679
NH_4^+ (ug m^{-3})	0.351	0.676	18.17	0.180	0.096	0.415
NO_3^- (ug m^{-3})	0.187	0.456	10.925	0.042	0.004	0.189
Cl^- (ug m^{-3})	0.166	1.271	53.270	0.029	0.016	0.076
PNC (cm^{-3})	8182	19031	40300	2032	2032	8335
Mode diameter (nm)	104	31	-	102	85	122
Geom. SD	1.71	0.13	-	1.70	1.65	1.75

In order to demonstrate the influence of close fires and the changing inversion layer, the time series of major greenhouse gases (CO, CO_2, CH_4 and N_2O), gaseous elemental mercury, acetonitrile and ozone throughout the campaign are shown in Figure 5. Sub-micron non-refractory aerosol organic, sulfate, ammonium and nitrate mass

Atmos. Chem. Phys. Discuss., doi:10.5194/acp-2016-866, 2016
Manuscript under review for journal Atmos. Chem. Phys.
Published: 10 November 2016

concentrations, organic mass fraction, PM_1 OC and EC mass concentrations and particle size distributions for the sampling period are shown in Figure 6. Periods of missing data correspond to times when instruments were not operating. Most of these time series display a clear diurnal trend as a result of the varying inversion layer height. Other enhancements in concentrations can be clearly seen and correspond to periods of frequent close fires (Figure 2). Over the entire sampling period from the 29th of May 2014 until the 28th of June 2014, four biomass burning related periods (BBP) and a "coastal" period (CP) have been distinguished. The dates for these periods are shown in Table 2. These periods are also displayed in Figure 5 and Figure 6.

Table 2 The start and end dates for the four identified Biomass Burning Periods (BBP1, BBP2, BBP3 and BBP4) and the Coastal Period (CP).

Period	Start date (mm/dd/yy hh:mm)	End date (mm/dd/yy hh:mm)
BBP1	05/30/14 00:00	05/31/14 23:59
BBP2	06/06/14 00:00	06/12/14 23:59
BBP3	06/14/14 00:00	06/17/14 23:59
CP	06/19/14 12:00	06/22/14 23:59
BBP3	06/23/14 00:00	06/28/14 23:59

Atmos. Chem. Phys. Discuss., doi:10.5194/acp-2016-866, 2016
Manuscript under review for journal Atmos. Chem. Phys.
Published: 10 November 2016

Atmospheric Chemistry and Physics
Discussions

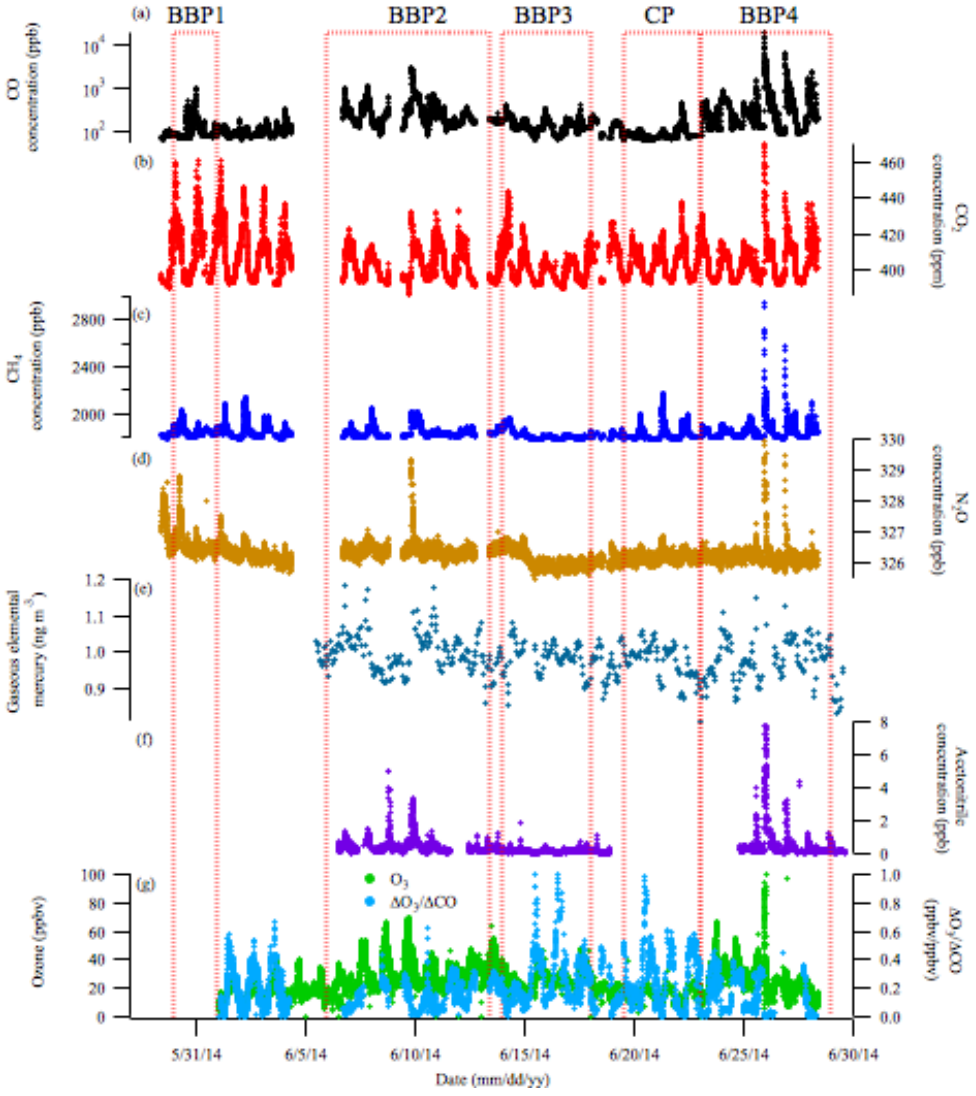

Figure 5 The time series of the major measured gaseous species during the SAFIRED campaign: (a) carbon monoxide, (b) carbon dioxide, (c) methane, (d) nitrogen dioxide, (e) gaseous elemental mercury, (f) acetonitrile and (g) ozone and $\Delta O_3/\Delta CO$. The biomass burning and coastal periods are indicated by the red dotted lines. All parts-per notation refer to mole fractions unless otherwise indicated.

Atmos. Chem. Phys. Discuss., doi:10.5194/acp-2016-866, 2016
Manuscript under review for journal Atmos. Chem. Phys.
Published: 10 November 2016

Atmospheric Chemistry and Physics Discussions
Open Access

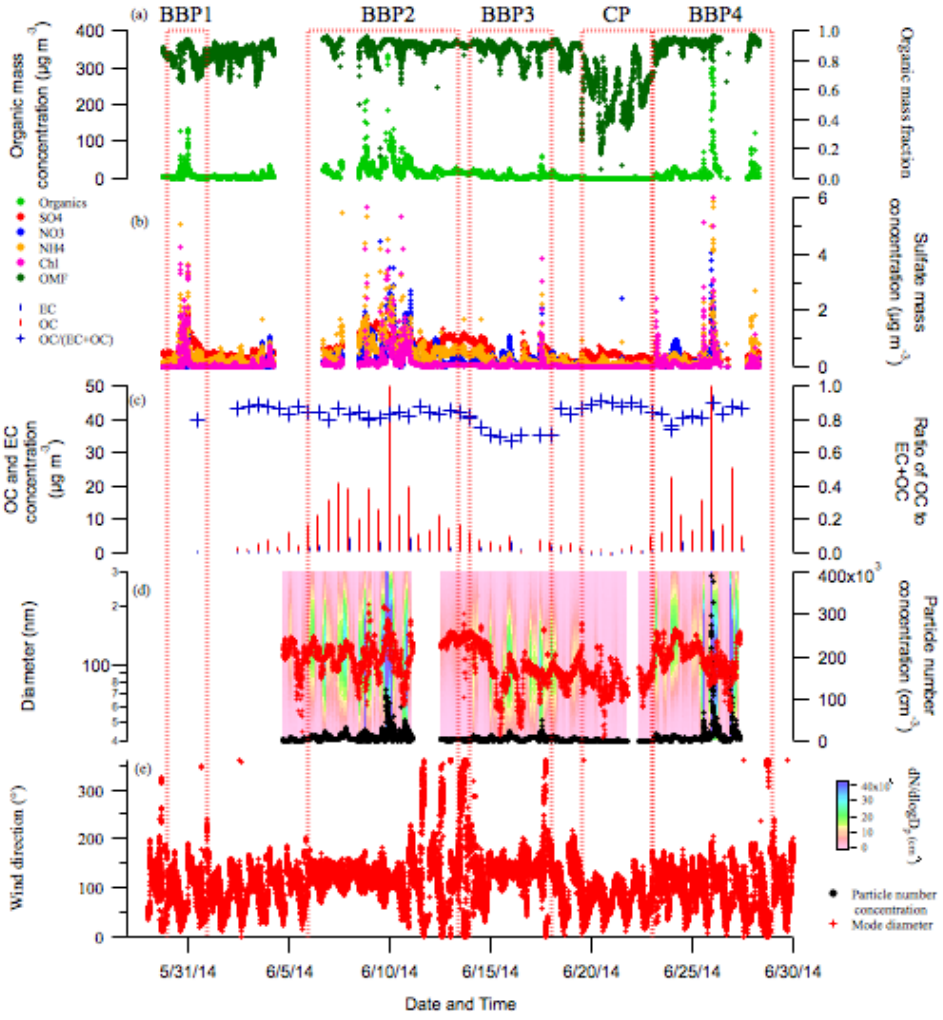

Figure 6 The times series of the major aerosol properties during the SAFIRED campaign: (a) the non-refractory PM_1 organic mass concentration (left) and organic mass fraction (right), b) the inorganic non-refractory PM_1 mass concentrations, (c) the 12-hour filter OC and EC PM_1 mass concentrations (left) and the ratio of OC to OC+EC (right), (d) the particle size distributions and particle size mode (left) and the total particle number concentration (right) and (e) the wind direction at ATARS.

Over the campaign organics dominated the non-refectory sub-micron aerosol mass contributing, on average 90% (median; 86%) of the total mass. Sulphate, nitrates, ammonium and chloride species contributed the rest of this mass, with the largest contributions from sulphate and ammonium. Sulphate contributions were very significant during the coastal period, contributing up to 32% of the total mass. Although

Atmos. Chem. Phys. Discuss., doi:10.5194/acp-2016-866, 2016
Manuscript under review for journal Atmos. Chem. Phys.
Published: 10 November 2016

chlorides contributed the least to the total mass, on average, during clear biomass burning events where sharp increases in CO and organics were observed, chlorides made up the largest component of inorganic aerosol. The maximum chloride concentration during the campaign reached 53 µg m^{-3}. High soil and vegetation chloride contents have been observed in savannah and coastal environments (Lobert et al., 1999;Andreae et al., 1996). The strong elevations of chloride signals observed, particularly during burning events BBP1, BBP2 and BBP4 are likely a result of emission of these chloride ions. Outside of the "burning events" where very sharp increases in concentrations were observed, chloride concentrations were very low. This either suggests that these chloride species are short-lived, or only present in fires very close to the coast and therefore the ATARS site.

Particle size distributions were unimodal for the majority of the sampling period with a mode of approximately 100 nm on average (see Figures 6d and 7). The SMPS was not operational during BBP1. Although the shape of the BBP4 size distribution was similar to the campaign average, concentrations were much higher and a result of close fires. BBP2 had a slightly larger size distribution centered on 110 nm. The size distribution during BBP3 was slightly smaller than the campaign average and BBP2 and BBP4, with a mode centered on ~95 nm. The contrast between these size distributions could be a result of atmospheric aging and dilution in which organic mass condenses onto or evaporates from the particle. Variations in fuel load or burning conditions could also contribute to this difference. The size and concentration of particles during the Coastal Period (CP) were much smaller than the rest of the campaign. There were two periods during CP where a bimodal size distribution was observed; one from approximately 3 pm until midnight on the 19th of June and the other

Atmos. Chem. Phys. Discuss., doi:10.5194/acp-2016-866, 2016
Manuscript under review for journal Atmos. Chem. Phys.
Published: 10 November 2016

between 2 pm and 6 pm on the 20th of June. As mentioned earlier, air masses during this time had a stronger oceanic influence, with back trajectories in this period originating along the east coast of Australia and passing over very little land before arriving at the station. The size distributions for both of these periods had a mode at approximately 20 nm and another at approximately 85 nm. Submicron sulfates made up to 32% of the total submicron non-refractory mass concentrations, as reported by the cToF-AMS from the period of midday on the 19th of June until midnight on the 22nd of June, whereas the average sulfate contribution for the rest of the campaign was approximately 8%. The low radon fetch, small particle concentrations, bimodal size distributions and significant contributions of sulfate during this period suggest very little biomass burning signal and a more marine-like aerosol. No particle nucleation events were observed over the entire sampling period (See Supplementary Figure S2). This is likely due to the elevated particle concentrations acting as a condensation sink.

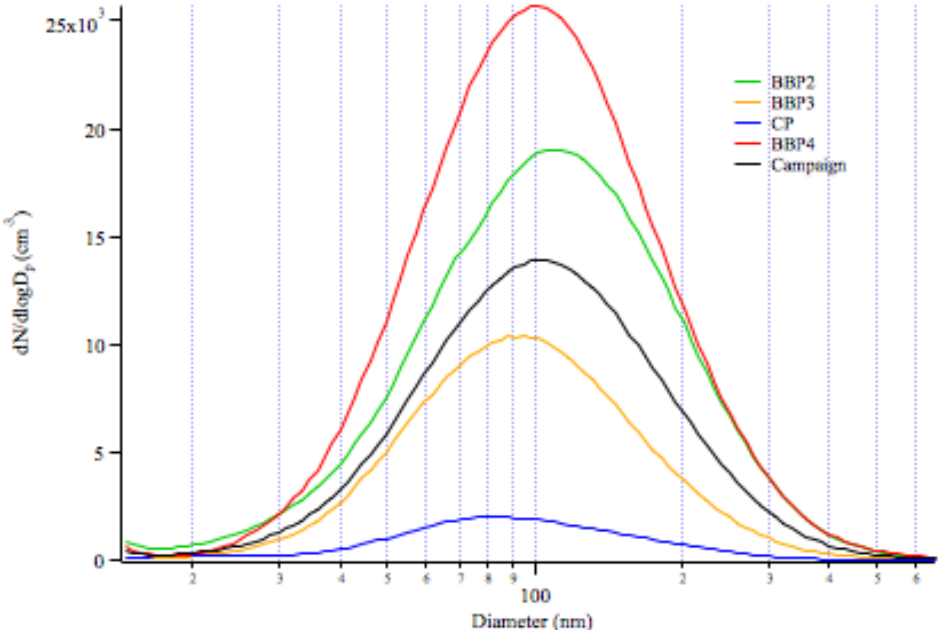

Figure 7 The average size distribution during BBP2, BBP3, BBP4, CP and the campaign average. The SMPS was not operational during BBP1.

Atmos. Chem. Phys. Discuss., doi:10.5194/acp-2016-866, 2016
Manuscript under review for journal Atmos. Chem. Phys.
Published: 10 November 2016

BBP1, BBP2 and BBP4 correspond to the periods when fires were burning within 10 km of ATARS. Large enhancements of biomass burning related emissions were observed during these three periods. There were distinct enhancements of all measured gaseous and aerosol species during these periods. Differences between the maximum and background concentrations were very prominent for CO (note the logarithmic scale in Figure 5a), CH_4, N_2O, acetonitrile (an established marker for biomass burning) and organic, nitrate and chloride non-refractory sub-micron aerosol species. Similar enhancements of CH_4 were also observed outside of these BB periods, which suggests another source of methane in this region. Only slight enhancements of GEM concentrations above background were observed during BBP2 and BBP4. Similar to much of the rest of the campaign sampling period, the non-refractory submicron aerosol was dominated by organics, with contributions typically varying between 70% and 95% of the mass. Relative to background concentrations, there were also large enhancements of nitrate and chloride species during these periods. While there were also enhancements of sulfate and ammonium species during these periods, similar enhancements were observed outside of these periods, again indicating a non-fire source of these species. The ratio of O_3 to CO concentrations above background (taken as 10 ppbv and 66 ppbv, respectively) gives an indication of the photochemical age of a smoke plume. $\Delta O_3/\Delta CO$ were lowest during BBP2 and BBP4 (and not measured during BBP1) relative to the rest of the campaign, indicating that the biomass burning signals during these periods had not undergone extensive photochemical aging and are therefore characteristic of fresh smoke.

Elevated signals during BBP1 were likely a result of a series of close fires within 5 km ENE of ATARS. The VIIRS and MODIS sensors on the SUMO NPP, Terra and Aqua

Atmos. Chem. Phys. Discuss., doi:10.5194/acp-2016-866, 2016
Manuscript under review for journal Atmos. Chem. Phys.
Published: 10 November 2016

Atmospheric Chemistry and Physics Discussions

satellites observes smaller fires at approximately 2 pm on the 30th of May. Winds were northeasterly during these two events. It is therefore likely that these signals were continuation or evolution of those fires. Burned vegetation was also visually observed the next morning at these locations. The large burst event later on the evening of the 31st of May is unlikely to be associated with these fires as the wind direction during this event was from the SSW and SSE. Large clusters of fires were observed at approximately 100 km and 150 km SE of the station by the Terra and Aqua satellites. The signals observed during this event could be a result of the plumes from this fire, although the possibility of a fire ignited after the satellite flyovers, or a combination of these cannot be eliminated.

Large signal enhancements on the 8th of June during BBP2 is likely a result of a cluster of fires approximately 100 km south east of the station. The MODIS sensors on the Terra and Aqua satellites observed the small cluster of fires along the back-trajectory at 11:14 am and 1:56 pm. The source of BB emissions for the large event on the 9th of June during this period is unclear. Several fires approximately 5 km from the station along the back-trajectory were detected by the MODIS sensor on Aqua and the VIIRS sensor on SUOMI NPP at approximately 2:30 pm on the 9th of June. There were also numerous fires detected between 100 km and 200 km southeast along this trajectory. The signals associated with this event could therefore be a result of the closer fires that started to blaze later in the evening, the distant fires or a combination of both.

Only one fire within 20km of ATARS was observed during BBP3 on the 17th of June. Numerous fires were observed further than 20km from the station and is possible that the signals during this period were more aged. While photochemical aging and

Atmos. Chem. Phys. Discuss., doi:10.5194/acp-2016-866, 2016
Manuscript under review for journal Atmos. Chem. Phys.
Published: 10 November 2016

coagulation typically lead to larger particles, particle size distributions were smaller during this period and the ratio of OC to OC+EC was 70%, 10% lower than the ratio during the rest of the campaign. Whether these observations were a result of burn conditions or aging processes (i.e. evaporation of organic compounds from the aerosol phase) is unclear, although the highest $\Delta O_3/\Delta CO$ values during the campaign were observed during BBP3, which indicates photochemical aging was more extensive during this period.

One close fire was also observed during CP, however wind directions during this period were typically north-easterly and concentrations were therefore much lower. 5-day HYSPLIT trajectories also show that air mass during the CP originated along the east coast of Australia before travelling towards the sampling station with very little terrestrial influence.

Close proximity fires

With numerous fires occurring across the region and the limitations of once-per-day satellite fly-overs and stationary measurements, it can be difficult to identify the exact source of these elevated signals. For a portion of BBP4, however, fires were burning within several kilometers of ATARS and several plumes were easily observed from the station. The signals from these plumes are shown in Figure 8. The observed enhancements between 12:30 pm and 3:00 pm on the 25th June during BBP4 were a result of grass fires burning approximately 1 km south-east from the station. During this event, the wind direction (Figure 8k) was highly variable, changing between 140° and 80° True Bearing (TB) multiple times. As a result, the sampling changed from measuring the air mass with and without the plume from this fire, which led to sharp increases and decreases in biomass burning-related signals (Figure 8a through 8j).

Atmos. Chem. Phys. Discuss., doi:10.5194/acp-2016-866, 2016
Manuscript under review for journal Atmos. Chem. Phys.
Published: 10 November 2016

Visually, the fire area and extent of the plume was larger at 4:00pm than earlier, however the wind direction changed to north-easterly which directed the plume away from the station. From 4:00 pm until 10:00 pm, the wind direction was stable at approximately 50° TB. At 10:00 pm, the wind direction rapidly changed to directly south and the largest enhancements for the whole campaign were observed until approximately 2:00 am on the 26th of June. It is very likely that these signals were a result of a continuation and evolution of these fires as the night progressed. Portions of a ~0.25 km^2 grassland field within 500 m directly south of ATARS were observed to be burned upon arrival at the station on the morning of the 26th of June and we speculate that the burning of this field contributed to the large enhancements in measured biomass burning emissions. The emissions during this portion of BBP4 are likely to be the most representative of fresh biomass burning smoke during the SAFIRED campaign.

Atmos. Chem. Phys. Discuss., doi:10.5194/acp-2016-866, 2016
Manuscript under review for journal Atmos. Chem. Phys.
Published: 10 November 2016

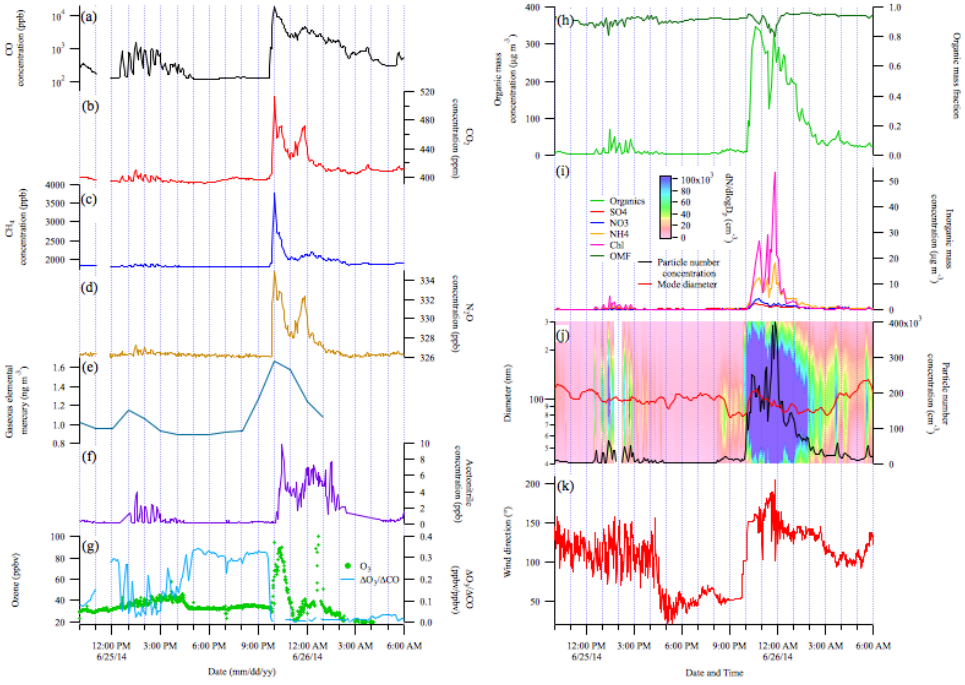

Figure 8 The major gas and aerosol concentrations measured during two biomass burning events within 1 km of ATARS during BBP4. (a) through (g) and (h) through (k) are as per Figures 5 and 6, respectively. All parts-per notation or mole fractions unless otherwise indicated.

4. Outcomes of SAFIRED

The overall aim of this study was to investigate the characteristics of BB emissions in the tropical savannah region of northern Australia during the early dry season. For many gaseous and aerosol species, elevated signals were observed for much of the month-long sampling period due to the high frequency of fires. The more specific outcomes of SAFIRED are outlined below.

Emission factors

Australian fires are responsible for 6% of global CO_2 biomass burning emissions, most of which is due to savannah fires (Shi et al., 2015). Carbon sequestering during regrowth periods is considered to balance carbon emissions in tropical Australia

(Haverd et al., 2013). Greenhouse gases emitted from savannah fires that are not sequestered, such as methane (CH_4) and nitrous oxide (N_2O), have been shown to contribute 2-4% of the annual accountable greenhouse gas emissions from Australia (Meyer et al., 2012). Seasonal emission factors for the major greenhouse gases are important for national greenhouse gas inventories and in understanding the impact of savannah fires. Furthermore, emission factors of CO_2 and CO can be used to infer mechanisms behind the emissions of other species, such as the connection between particulate matter and burning conditions.

The gaseous and aerosol data for the sample period were investigated to identify BB events and determine the emission factors of CO_2, CO, CH_4. N_2O, as well as Aitken and Accumulation mode aerosols and submicron particle species (organics, sulfates, nitrates, ammonium and chlorides) for several individual BB events. These emission factors were mostly found to be dependent on the combustion conditions (using the modified combustion efficiency as a proxy) of the fires. These results will be the first set of emission factors for aerosol particles from savannah fires in Australia. Furthermore, the variability in emission factors for different fires calls for a separation of single-value emission factors that are usually reported for savannah fires into grass and shrub components. A full discussion of these results are presented in Desservettaz et al. (2016, submitted).

Non-methane organic compounds (NMOCs)

Biomass burning is the second largest source of NMOCs globally with a recent global estimate of at least 400 Tg year^{-1}, second only to biogenic sources (Akagi et al., 2011). Biomass burning produces a complex mix of NMOCs, which may be saturated or unsaturated, aliphatic or aromatic, and contain substitutions of oxygen, sulfur, nitrogen,

halogens and other atoms. NMOC emission rates are strongly tied to the efficiency of combustion, with smouldering fires emitting NMOC at higher rates than flaming fires (Andreae and Merlet, 2001). Biomass burning derived NMOCs fuel the production of tropospheric ozone in diluted, aged biomass burning plumes, with higher ozone enhancements observed when biomass burning plumes interact with NOx-rich urban plumes (Jaffe and Wigder, 2012;Wigder et al., 2013;Akagi et al., 2013). Oxidation of NMOCs results in lower volatility products that partition to the aerosol phase and contribute significantly to secondary organic aerosol (Hallquist et al., 2009). Biomass burning produces significant amounts of semi-volatile NMOC which can be difficult to quantify and identify with current measurement techniques. However recent studies have shown that including semi volatile NMOC chemistry in models improves the agreement between the modeled and observed organic aerosol (Alvarado et al., 2015; Konovalov et al., 2015) and ozone (Alvarado et al., 2015). High quality NMOC emission factors are crucial for models to assess the impact of biomass burning plumes on air quality and climate.

PAHs

Polycyclic aromatic hydrocarbons (PAHs) are a group of chemicals that are formed and emitted during combustion processes. Globally, major sources include residential/commercial biomass burning, open-field biomass burning and vehicular emissions (Shen et al., 2013). In Oceania in 2007, 31% of PAH emissions were estimated to be attributed to deforestation and wildfires (Shen et al., 2013). With control strategies targeting and reducing vehicular emission of PAHs over the last few decades, the relative contribution of other emission sources, such as savannah fires, has increased (Friedman et al., 2013;Kallenborn et al., 2012;Wang et al., 2016). Although most of these emissions are in the gas-phase (Jenkins et al., 1996;Atkins et al., 2010), the

Atmos. Chem. Phys. Discuss., doi:10.5194/acp-2016-866, 2016
Manuscript under review for journal Atmos. Chem. Phys.
Published: 10 November 2016

particle-phase PAHs, such as benzo[a]pyrene (BaP), may have high genotoxicity (IARC., 2015). However, field-based studies on emissions of PAHs from open-field biomass burning, including savannah fires remain limited in Australia (Freeman and Cattell, 1990).

Emission factors of PAHs from biomass burning related to savannah fires in northern Australia will be estimated form the data collected during this campaign. This estimation will be based on the (background subtracted) concentrations of PAHs and CO_2 (and CO) during the events where biomass burning contributes most to these concentrations measured at the sampling site. The concentrations of 13 major PAHs (gaseous plus particle-associated phase) varied from ~ 1 to over 15 ng m^{-3} within different BB events. In the gas phase, 3- and 4-ring compounds typically contributed ~ 90% to the sum concentrations whereas the particle-associated PAHs were dominated by 5- and 6-ring compounds (> 80%). Measured PAH concentrations were significantly higher (paired *t*-test, $P < <0.05$) during BB events E, F and G. For these events, concentrations of BaP exceeded the monitoring investigation level for atmospheric BaP in Australia (National-Environment-Protection-Council-Service-Corporation, 2011), i.e. 0.30 ng m^{-3}, by 66% (BB event E) and 200% (BB events F and G). A full discussion of these results can be found in (Wang et al., 2016, under review).

Mercury

The atmosphere is the dominant transport pathway for mercury globally, with emissions to the atmosphere from both natural and anthropogenic origins (Driscoll et al., 2013). Whilst our understanding of the natural cycling of mercury has improved markedly over the past decades (Pirrone et al., 2010), large uncertainties still exist; specifically, global emission estimates to the atmosphere from biomass burning currently range between

Atmos. Chem. Phys. Discuss., doi:10.5194/acp-2016-866, 2016
Manuscript under review for journal Atmos. Chem. Phys.
Published: 10 November 2016

300 and 600 Mg year^{-1} (Driscoll et al., 2013). In the atmosphere, mercury exists as one of three operationally-defined species: gaseous elemental mercury (GEM), gaseous oxidised mercury (GOM) and particulate-bound mercury (PBM), each with differing abundances, solubility and depositional characteristics and with in-air conversion between all three species possible (Lin and Pehkonen, 1999). Mercury can be scavenged from the atmosphere through both wet and dry depositional processes, and the monsoonal climate of northern Australia results in varying significance of each of these processes through the year (Packham et al., 2009). Upon deposition, mercury may be stored in plant tissue via stomatal or cuticular uptake (Rea et al., 2002) or sequestered within soils (Gustin et al., 2008). Release from both of these pools is achieved from burning events that may volatilise or thermally desorb mercury from biomass and soil, respectively (Melendez-Perez et al., 2014). Subsequently this mercury pool is redistributed through the atmospheric pathway to ecosystems that may methylate mercury, thereby enhancing its bioavailability to the local food chain.

SAFIRED represents the first measurements of atmospheric mercury undertaken in the tropical region of the Australian continent. The mean observed GEM concentration over the study period was 0.99 ± 0.09 ng m^{-3}, similar to the average over that month (0.96 ng m^{-3}) for 5 other Southern Hemisphere sites and slightly lower than the average (1.15 ng m^{-3}) for 5 tropical sites (Sprovieri et al., 2016). Mean GOM and PBM concentrations were 11 ± 5 pg m^{-3} and 6 ± 3 pg m^{-3} respectively, representing 0.6 – 3.4% of total observed atmospheric mercury.

Atmospheric mercury measurements were available only during the final four identified burn events. During these events, spikes in GEM concentrations were observed, though

Atmos. Chem. Phys. Discuss., doi:10.5194/acp-2016-866, 2016
Manuscript under review for journal Atmos. Chem. Phys.
Published: 10 November 2016

there were no significant increases in GOM or PBM. Emission ratios calculated during the campaign were two orders of magnitude higher than those reported by Andreae and Merlet (2001), though those were from scrub, rather than grass, BB events (Desservettaz et al., 2016). Future outcomes from the SAFIRED campaign will focus on the use of micrometeorological techniques and the passive tracer radon to quantify delivery of atmospheric mercury to tropical savannah ecosystems. ATARS also now serves as an additional site measuring continuous GEM as part of the Global Mercury Observation System (GMOS), one of only two tropical observing sites in the Eastern Hemisphere and the third such site located in Australia.

Aging of aerosols

Atmospheric chemistry and radiative forcing will depend on how gaseous and aerosol emissions from fires age as they move and interact with each other and existing species in the atmosphere. Biomass burning aerosols can be involved in condensation and coagulation (Radhi et al., 2012), undergo water uptake (Mochida and Kawamura, 2004) form cloud droplets (Novakov and Corrigan, 1996), and be exposed to photochemical aging processes, including those involving the gaseous components of fire emissions (Keywood et al., 2011;Keywood et al., 2015). With a reported lifetime of 3.8 ± 0.8 days (Edwards et al., 2006), biomass burning aerosols are able to travel intercontinental distances (Rosen et al., 2000) and are therefore present in the atmosphere long enough for substantial changes due to aging. Furthermore, tropical convection is likely to affect the aging of BB emissions in the region around ATARS, due to the immediate proximity to the warm waters in the Timor Sea (Allen et al., 2008). This introduces further uncertainty to the effect of BB emissions on radiation flux.

Atmos. Chem. Phys. Discuss., doi:10.5194/acp-2016-866, 2016
Manuscript under review for journal Atmos. Chem. Phys.
Published: 10 November 2016

Primary organic aerosol directly emitted from biomass burning can interact with NMOCs to change composition and mass, resulting in secondary organic aerosol (Hallquist et al., 2009). Photochemical oxidation of NMOCs occurs during the daytime by either hydroxyl radicals or ozone. Ozone is also typically produced in the aging processes of tropical biomass burning plumes when NMOCs can oxidise to produce peroxy radicals that react with NO. Photochemical reactions also may lead to an overall increase in total aerosol mass through the condensation of NMOCs onto existing particles (Reid et al., 1998;Yokelson et al., 2009;Akagi et al., 2012;DeCarlo et al., 2008). Some studies have shown the opposite, i.e., photo-oxidation can also lead to the evaporation of some primary organic constituents, resulting in an overall mass reduction (Hennigan et al., 2011;Akagi et al., 2012). With thousands of organic compounds in the atmosphere, each with different volatilities and potential reaction mechanisms, our understanding of secondary organic aerosol production is limited (Goldstein and Galbally, 2007;Keywood et al., 2011). Furthermore, secondary organic aerosol can also form through aqueous phase reactions where water-soluble organics dissolve into water on existing particles (Lim et al., 2010).

Further analysis into the aerosol chemical composition will elucidate the aging of early dry season biomass burning emissions. Fractional analysis (e.g., f44 and f60, the fraction of m/z 44 and m/z 60 to all organic masses, indicated oxygenation and BB sources, respectively) and factor analysis using positive matrix factorisation (PMF) of cToF-AMS data has been investigated over the entire sampling period. Outside of the periods of significant influence from BB events, three PMF-resolved organic aerosol factors were identified. A BB organic aerosol factor was found to comprise 24% of the submicron non-refractory organic mass, with an oxygenated organic aerosol factor and

Atmos. Chem. Phys. Discuss., doi:10.5194/acp-2016-866, 2016
Manuscript under review for journal Atmos. Chem. Phys.
Published: 10 November 2016

a biogenic isoprene-related secondary organic aerosol factor comprising 47% and 29%, respectively. These results indicate the significant influence of fresh and aged BB on aerosol composition in the early dry season. The emission of precursors from fires is likely responsible for some of the SOA formation. A full discussion of these results can be found in Milic et al. (2016). Future analysis will investigate the gas and particle-phase composition for individual BB events.

Water uptake of aerosols

The water uptake by aerosols is determined by their size and composition, as well as the atmospheric humidity (McFiggans et al., 2006). The hygroscopic properties of all of the different components of an aerosol particle contribute to its total hygroscopicity (Chen et al., 1973;Stokes and Robinson, 1966). The presence of different water-soluble and water-insoluble organics and inorganics will therefore strongly influence water uptake. Furthermore, chamber studies that have investigated emissions from biomass fuels, both separately and in combination, have shown that the hygroscopic response can vary significantly depending on fuel type (Carrico et al., 2010). Understanding the water uptake of atmospheric aerosols is further complicated when considering other aging processes as described previously. Nonetheless, it is important to characterise the water uptake, as this will, in turn, influence other atmospheric chemistry processes, radiation scattering and absorption as well as cloud processing.

Biomass burning aerosols can act as cloud condensation nuclei if they are large enough for water to easily condense onto their surface, or if the particles have a large affinity for water due to their composition (Novakov and Corrigan, 1996). Ultimately, this means that BB emissions can lead to a higher number of cloud droplets. This is important in reflecting solar radiation and cooling the earth's surface. Cloud albedo is

Atmos. Chem. Phys. Discuss., doi:10.5194/acp-2016-866, 2016
Manuscript under review for journal Atmos. Chem. Phys.
Published: 10 November 2016

more susceptible to changes when cloud condensation nuclei concentrations are relatively low (Twomey, 1991), such as in marine environments like the Timor Sea off the coast of northern Australia.

The water uptake of aerosols has been further investigated to identify the possible influence of early dry season BB in this region on cloud formation. The concentrations of cloud condensation nuclei at a constant supersaturation of 0.5% were typically of the order of 2000 cm^{-3} and reached well over 10000 cm^{-3} during intense BB events. Variations in the ratio of aerosol particles activating cloud droplets showed a distinct diurnal trend, with an activation ratio of 40% ± 20% during the night and 60% ± 20% during the day. The particle size distribution and the hygroscopicity of the particles were found to significantly influence this activation ratio. A full discussion of these results can be found in Mallet et al. (2016, submitted). Future analysis will elucidate the contribution of different biomass burning aerosol components on the hygroscopicity.

Trace metal deposition

The deposition and dissolution of aerosols containing trace metals into the ocean may provide important micronutrients required for marine primary production. Conversely, the deposition of soluble iron can trigger toxic algal blooms, such as Trichodesmium, in nutrient-poor tropical and subtropical waters (LaRoche and Breitbarth, 2005). Trichodesmium blooms require large quantities of soluble iron, of which aerosols are a source (Boyd and Ellwood, 2010;Rubin et al., 2011). To date, most studies have assumed that mineral dust aerosols represent the primary source of soluble iron in the atmosphere (Baker and Croot, 2010); however fire emissions and oil combustion are other likely sources (Ito, 2011;Schroth et al., 2009;Sedwick et al., 2007). A few studies

have shown that iron contained in biomass burning emissions is significantly more soluble than mineral dust (Guieu et al., 2005;Luo et al., 2008;Schroth et al., 2009) but, to date, no data exists for Australian fires.

The aim of the trace metal aerosol component of SAFIRED is to quantify, for the first time, the fractional solubility of aerosol iron, and other trace metals, derived from Australian dry season BB. The fractional iron solubility is an important variable determining iron availability for biological uptake. On a global scale, the large variability in the observed fractional iron solubility results, in part, from a mixture of different aerosol sources. Estimates of fractional iron solubility from fire combustion (1 - 60 %) are thought to be greater than those originating from mineral dust (1 - 2%) (Chuang et al., 2005;Guieu et al., 2005;Sedwick et al., 2007), and may vary in relationship to biomass and fire characteristics as well as that of the underlying terrain (Paris et al., 2010;Ito, 2011). Iron associated with BB may provide information with respect to BB inputs of iron to the ocean (Giglio et al., 2013;e.g. Meyer et al., 2008). The ATARS provides an ideal location to further investigate BB derived fractional iron solubility at the source. The results from this study can be found in Winton et al. (2016) and show that soluble iron concentrations from BB sources are significantly higher than those observed in Southern Ocean baseline air masses from the Cape Grim Baseline Air Pollution Station, Tasmania, Australia (Winton et al., 2015). Aerosol iron at SAFIRED was a mixture of fresh BB, mineral dust, sea spray and industrial pollution sources. The fractional iron solubility (2 - 12%) was relatively high throughout the campaign and the variability was related to the mixing and enhancement of mineral dust iron solubility with BB species.

Atmos. Chem. Phys. Discuss., doi:10.5194/acp-2016-866, 2016
Manuscript under review for journal Atmos. Chem. Phys.
Published: 10 November 2016

5. Looking forward

While the specific outcomes of the SAFIRED campaign are reviewed above, the general importance of this study can be discussed in a greater context. This is the first large-scale collaborative project undertaken in this region and draws on the resources and expertise of most of Australia's research institutes focused on atmosphere chemistry and composition. Large scale, multidisciplinary measurement campaigns in the tropics, such as SAFIRED, are needed to make distinctions between different types of fires in different regions to reduce uncertainties in global climate models (Keywood et al., 2013). This need has been recognized with the formation of global collaborative initiatives promoting interdisciplinary collaboration in biomass burning research (Kaiser and Keywood, 2015). As the world moves towards a warmer climate, biomass burning is likely to increase in frequency and intensity, and these emissions will become an increasingly important source of trace gases and aerosols to the atmosphere. SAFIRED lays the foundation for future measurements at ATARS that could make measurements throughout the whole dry season and on a more long-term scale. Future work in this region should focus on 1) the detailed characterisation of individual fires and their emissions, 2) biomass burning emissions throughout the late dry season and 3) the vertical and horizontal transport of biomass burning emissions in this region.

Data availability

All data are available upon request from the corresponding authors (Branka Miljevic, b.miljevic@qut.edu.au; Melita D. Keywood; melita.keywood@csiro.au).

Atmos. Chem. Phys. Discuss., doi:10.5194/acp-2016-866, 2016
Manuscript under review for journal Atmos. Chem. Phys.
Published: 10 November 2016

Author Contributions

M.D. Mallet[a,b,c,d,e], M.J. Desservettaz[b,c,d,e], B. Miljevic[b,c,e*], A. Milic[b,d,e], Z.D. Ristovski[b,e], J. Alroe[b,c,e], L.T. Cravigan[b,c,e], E.R. Jayaratne[d,e], C. Paton-Walsh[b,c,e], D.W.T. Griffith[b,d,e], S.R. Wilson[b,d,e], G. Kettlewell[b,e], M.V. van der Schoot[b,e], P. Selleck[b,c,d,e], F. Reisen[b,c,e], S.J. Lawson[b,c,d,e], J. Ward[b,c,d,e], J. Harnwell[b,c,e], M. Cheng[b,c,d,e], R.W. Gillett[b,c,d,e], S.B. Molloy[d,e], D. Howard[b,c,d,e], P.F. Nelson[b,e], A.L Morrison[b,e], G.C. Edwards[b,c,e], A.G. Williams[b,c,e], S.D. Chambers[b,c,d,e], S. Werczynski[b,c,e], L.R. Williams[c,d,e], V.H.L. Winton[b,c,d,e], and B. Atkinson[b,c], X. Wang[b,d,e], M.D. Keywood[b,c,d,e,f*]

a: Wrote and organised the manuscript

b: Contributed to the organisation of the campaign

c: Installed and/or operated instrumentation during the sampling period

d: Analysed data

e: Contributed to the manuscript and/or data interpretation

f: Designed and led the campaign.

*: Corresponding author

Competing interests

The authors declare that they have no conflict of interest.

Acknowledgements

The majority of the campaign was internally funded. The input of QUT was supported by the Australian Research Council Discovery (Grant DP120100126). The work on aerosol iron solubility was supported by Curtin University (RES-SE-DAP_AW-47679-

1), the University of Tasmania (B0019024) and the Australian Research Council (Grant FT130100037).

6. References

Akagi, S., Yokelson, R. J., Wiedinmyer, C., Alvarado, M., Reid, J., Karl, T., Crounse, J., and Wennberg, P.: Emission factors for open and domestic biomass burning for use in atmospheric models, Atmospheric Chemistry and Physics, 11, 4039-4072, 2011.

Akagi, S., Yokelson, R. J., Burling, I. R., Meinardi, S., Simpson, I., Blake, D. R., McMeeking, G., Sullivan, A., Lee, T., and Kreidenweis, S.: Measurements of reactive trace gases and variable O_3 formation rates in some South Carolina biomass burning plumes, Atmospheric Chemistry and Physics, 13, 1141-1165, 2013.

Akagi, S. K., Craven, J. S., Taylor, J. W., McMeeking, G. R., Yokelson, R. J., Burling, I. R., Urbanski, S. P., Wold, C. E., Seinfeld, J. H., Coe, H., Alvarado, M. J., and Weise, D. R.: Evolution of trace gases and particles emitted by a chaparral fire in California, Atmospheric Chemistry and Physics, 12, 1397-1421, 2012.

Allen, G., Vaughan, G., Bower, K., Williams, P., Crosier, J., Flynn, M., Connolly, P., Hamilton, J., Lee, J., and Saxton, J.: Aerosol and trace-gas measurements in the Darwin area during the wet season, Journal of Geophysical Research: Atmospheres (1984–2012), 113, 2008.

Andersen, A. N., Cook, G. D., Corbett, L. K., Douglas, M. M., Eager, R. W., Russell-Smith, J., Setterfield, S. A., Williams, R. J., and Woinarski, J. C.: Fire frequency and biodiversity conservation in Australian tropical savannas: implications from the Kapalga fire experiment, Austral Ecology, 30, 155-167, 2005.

Andreae, M., Atlas, E., Harris, G., Helas, G., DeKock, A., Koppmann, R., Manõ, S., Pollock, W., Rudolph, J., and Scharffe, D.: Methyl halide emissions from savanna fires in southern Africa, 1996.

Andreae, M. O., and Merlet, P.: Emission of trace gases and aerosols from biomass burning, Global Biogeochemical Cycles, 15, 955-966, 2001.

Atkins, A., Bignal, K. L., Zhou, J. L., and Cazier, F.: Profiles of polycyclic aromatic hydrocarbons and polychlorinated biphenyls from the combustion of biomass pellets, Chemosphere, 78, 1385-1392, 2010.

Baker, A., and Croot, P.: Atmospheric and marine controls on aerosol iron solubility in seawater, Marine Chemistry, 120, 4-13, 2010.

Bindoff, N. L., Stott, P. A., AchutaRao, K. M., Allen, M. R., Gillett, N., Gutzler, D., Hansingo, K., Hegerl, G., Hu, Y., Jain, S., Mokhov, I. I., Overland, J., Perlwitz, J., Sebbari, R., and Zhang, X.: Detection and Attribution of Climate Change: from Global to Regional, in: Climate Change 2013: The Physical Science Basis. Contribution of Working Group I to the Fifth Assessment Report of the Intergovernmental Panel on Climate Change, edited by: Stocker, T. F., Qin, D., Plattner, G.-K., Tignor, M., Allen, S. K., Boschung, J., Nauels, A., Xia, Y., Bex, V., and Midgley, P. M., Cambridge University Press, Cambridge, United Kingdom and New York, NY, USA, 867–952, 2013.

Biraud, S., Ciais, P., Ramonet, M., Simmonds, P., Kazan, V., Monfray, P., O'Doherty, S., Spain, T. G., and Jennings, S. G.: European greenhouse gas emissions estimated

from continuous atmospheric measurements and radon 222 at Mace Head, Ireland, Journal of Geophysical Research: Atmospheres (1984–2012), 105, 1351-1366, 2000.

Boyd, P., and Ellwood, M.: The biogeochemical cycle of iron in the ocean, Nature Geoscience, 3, 675-682, 2010.

Carrico, C., Petters, M., Kreidenweis, S., Sullivan, A., McMeeking, G., Levin, E., Engling, G., Malm, W., and Collett Jr, J.: Water uptake and chemical composition of fresh aerosols generated in open burning of biomass, Atmospheric Chemistry and Physics, 10, 5165-5178, 2010.

Chambers, S., Williams, A., Crawford, J., and Griffiths, A.: On the use of radon for quantifying the effects of atmospheric stability on urban emissions, Atmospheric Chemistry and Physics, 15, 1175-1190, 2015.

Chambers, S. D., Hong, S.-B., Williams, A. G., Crawford, J., Griffiths, A. D., and Park, S.-J.: Characterising terrestrial influences on Antarctic air masses using Radon-222 measurements at King George Island, Atmospheric Chemistry and Physics, 14, 9903-9916, 2014.

Chambers, S. D., Williams, A. G., Conen, F., Griffiths, A. D., Reimann, S., Steinbacher, M., Krummel, P. B., Steele, L. P., van der Schoot, M. V., and Galbally, I. E.: Towards a Universal "Baseline" Characterisation of Air Masses for High-and Low-Altitude Observing Stations Using Radon-222, Aerosol Air Quality Research, 16, 885-899, 2016.

Chen, H., Sangster, J., Teng, T., and Lenzi, F.: A general method of predicting the water activity of ternary aqueous solutions from binary data, The Canadian Journal of Chemical Engineering, 51, 234-241, 1973.

Chow, J. C., Watson, J. G., Chen, L. W. A., Chang, M. C. O., Robinson, N. F., Trimble, D., and Kohl, S.: The IMPROVE-A temperature protocol for thermal/optical carbon analysis: maintaining consistency with a long-term database, Journal of the Air & Waste Management Association, 57, 1014-1023, 2007a.

Chow, J. C., Watson, J. G., Chen, L. W. A., Chang, M. O., Robinson, N. F., Trimble, D., and Kohl, S.: The IMPROVE-A temperature protocol for thermal/optical carbon analysis: maintaining consistency with a long-term database, Journal of the Air & Waste Management Association, 57, 1014-1023, 2007b.

Chuang, P. Y., Duvall, R. M., Shafer, M. M., and Schauer, J. J.: The origin of water soluble particulate iron in the Asian atmospheric outflow, Geophysical Research Letters, 32, L07813, 2005.

Crutzen, P. J., and Andreae, M. O.: Biomass burning in the tropics: Impact on atmospheric chemistry and biogeochemical cycles, Science, 250, 1669-1678, 1990.

DeCarlo, P. F., Dunlea, E. J., Kimmel, J. R., Aiken, A. C., Sueper, D., Crounse, J., Wennberg, P. O., Emmons, L., Shinozuka, Y., Clarke, A., Zhou, J., Tomlinson, J., Collins, D. R., Knapp, D., Weinheimer, A. J., Montzka, D. D., Campos, T., and Jimenez, J. L.: Fast airborne aerosol size and chemistry measurements above Mexico City and Central Mexico during the MILAGRO campaign, Atmospheric Chemistry and Physics, 8, 4027-4048, 2008.

Desservettaz, M. J., Paton-Walsh, C., Griffith, D. W. T., Kettlewell, G., Keywood, M. D., van der Schoot, M. V., Ward, J., Mallet, M. D., Milic, A., Miljevic, B., Ristovski, Z. D., Howard, D., Edwards, G. C., and Atkinson, B.: Emission factors of trace gases and particulates during the dry season in tropical northern Australia, Journal of Geophysical Research: Atmospheres, 2016, submitted.

Draxler, R. R., and Rolph, G.: HYSPLIT (HYbrid Single-Particle Lagrangian Integrated Trajectory) model access via NOAA ARL READY website (http://www/.

arl. noaa. gov/ready/hysplit4. html). NOAA Air Resources Laboratory, Silver Spring, in, Md, 2003.

Driscoll, C. T., Mason, R. P., Chan, H. M., Jacob, D. J., and Pirrone, N.: Mercury as a global pollutant: sources, pathways, and effects, Environmental science & technology, 47, 4967-4983, 2013.

Edwards, D., Emmons, L., Gille, J., Chu, A., Attié, J. L., Giglio, L., Wood, S., Haywood, J., Deeter, M., and Massie, S.: Satellite-observed pollution from Southern Hemisphere biomass burning, Journal of Geophysical Research: Atmospheres (1984–2012), 111, 2006.

Edwards, G. C., Rasmussen, P. E., Schroeder, W. H., Wallace, D. M., Halfpenny-Mitchell, L., Dias, G. M., Kemp, R. J., and Ausma, S.: Development and evaluation of a sampling system to determine gaseous Mercury fluxes using an aerodynamic micrometeorological gradient method, Journal of Geophysical Research: Atmospheres, 110, 2005.

Freeman, D. J., and Cattell, F. C. R.: Woodburning as a source of atmospheric polycyclic aromatic hydrocarbons, Environmental Science and Technology, 24, 1581-1585, 1990.

Friedman, C. L., Zhang, Y., and Selin, N. E.: Climate change and emissions impacts on atmospheric PAH transport to the Arctic, Environmental Science & Technology, 48, 429-437, 2013.

Giglio, L., Randerson, J. T., and Werf, G. R.: Analysis of daily, monthly, and annual burned area using the fourth-generation global fire emissions database (GFED4), Journal of Geophysical Research: Biogeosciences, 118, 317-328, 2013.

Goldstein, A. H., and Galbally, I. E.: Known and unexplored organic constituents in the earth's atmosphere, Environmental Science & Technology, 41, 1514-1521, 2007.

Govender, N., Trollope, W. S., and Van Wilgen, B. W.: The effect of fire season, fire frequency, rainfall and management on fire intensity in savanna vegetation in South Africa, Journal of Applied Ecology, 43, 748-758, 2006.

Griffith, D. W. T.: Synthetic calibration and quantitative analysis of gas-phase FT-IR spectra, Applied Spectroscopy, 50, 59-70, 1996.

Griffith, D. W. T., Deutscher, N. M., Caldow, C., Kettlewell, G., Riggenbach, M., and Hammer, S.: A Fourier transform infrared trace gas and isotope analyser for atmospheric applications, Atmos. Meas. Tech., 5, 2481-2498, 2012.

Guieu, C., Bonnet, S., Wagener, T., and Loÿe-Pilot, M. D.: Biomass burning as a source of dissolved iron to the open ocean?, Geophysical Research Letters, 32, 2005.

Gustin, M. S., Lindberg, S. E., and Weisberg, P. J.: An update on the natural sources and sinks of atmospheric mercury, Applied Geochemistry, 23, 482-493, 2008.

Hallquist, M., Wenger, J. C., Baltensperger, U., Rudich, Y., Simpson, D., Claeys, M., Dommen, J., Donahue, N. M., George, C., Goldstein, A. H., Hamilton, J. F., Herrmann, H., Hoffmann, T., Iinuma, Y., Jang, M., Jenkin, M. E., Jimenez, J. L., Kiendler-Scharr, A., Maenhaut, W., McFiggans, G., Mentel, T. F., Monod, A., Prevot, A. S. H., Seinfeld, J. H., Surratt, J. D., Szmigielski, R., and Wildt, J.: The formation, properties and impact of secondary organic aerosol: current and emerging issues, Atmospheric Chemistry and Physics, 9, 5155-5236, 2009.

Haverd, V., Raupach, M., Briggs, P., Canadell, J., Isaac, P., Pickett-Heaps, C., Roxburgh, S., van Gorsel, E., Viscarra Rossel, R., and Wang, Z.: Multiple observation types reduce uncertainty in Australia's terrestrial carbon and water cycles, Biogeosciences, 10, 2011-2040, 2013.

Hennigan, C. J., Miracolo, M. A., Engelhart, G. J., May, A. A., Presto, A. A., Lee, T., Sullivan, A. P., McMeeking, G. R., Coe, H., Wold, C. E., Hao, W. M., Gilman, J. B.,

Kuster, W. C., de Gouw, J., Schichtel, B. A., Collett, J. L., Kreidenweis, S. M., and Robinson, A. L.: Chemical and physical transformations of organic aerosol from the photo-oxidation of open biomass burning emissions in an environmental chamber, Atmospheric Chemistry and Physics, 11, 7669-7686, 2011.

Honninger, G., von Friedeburg, C., and Platt, U.: Multi axis differential optical absorption spectroscopy (MAX-DOAS), Atmospheric Chemistry and Physics, 4, 231-254, 2004.

Agents Classified by the IARC Monographs. World Health Organization. http://monographs.iarc.fr/ENG/Classification/, 2015.

Iinuma, Y., Engling, G., Puxbaum, H., and Herrmann, H.: A highly resolved anion-exchange chromatographic method for determination of saccharidic tracers for biomass combustion and primary bio-particles in atmospheric aerosol, Atmospheric Environment, 43, 1367-1371, 2009.

Ito, A.: Mega fire emissions in Siberia: potential supply of bioavailable iron from forests to the ocean, Biogeosciences, 8, 1679-1697, 2011.

Jacobson, M. Z.: Strong radiative heating due to the mixing state of black carbon in atmospheric aerosols, Nature, 409, 695-697, 2001.

Jaffe, D. A., and Wigder, N. L.: Ozone production from wildfires: A critical review, Atmospheric Environment, 51, 1-10, 2012.

Jenkins, B. M., Jones, A. D., Turn, S. Q., and Williams, R. B.: Emission Factors for Polycyclic Aromatic Hydrocarbons from Biomass Burning, Environmental Science & Technology, 30, 2462-2469, 1996.

Kaiser, J. W., and Keywood, M.: Preface for Atmos. Env. Special issue on IBBI, Atmospheric Environment, 121, 1-3, 2015.

Kallenborn, R., Halsall, C., Dellong, M., and Carlsson, P.: The influence of climate change on the global distribution and fate processes of anthropogenic persistent organic pollutants, Journal of Environmental Monitoring, 14, 2854-2869, 2012.

Keywood, M., Guyes, H., Selleck, P., and Gillett, R.: Quantification of secondary organic aerosol in an Australian urban location, Environmental Chemistry, 8, 115-126, 2011.

Keywood, M., Kanakidou, M., Stohl, A., Dentener, F., Grassi, G., Meyer, C. P., Torseth, K., Edwards, D., Thompson, A. M., Lohmann, U., and Burrows, J.: Fire in the air: Biomass burning impacts in a changing climate, Critical Reviews in Environmental Science and Technology, 43, 40-83, 2013.

Keywood, M., Cope, M., Meyer, C. M., Iinuma, Y., and Emmerson, K.: When smoke comes to town: The impact of biomass burning smoke on air quality, Atmospheric Environment, 121, 13-21, 2015.

Landis, M. S., Stevens, R. K., Schaedlich, F., and Prestbo, E. M.: Development and characterization of an annular denuder methodology for the measurement of divalent inorganic reactive gaseous mercury in ambient air, Environmental science & technology, 36, 3000-3009, 2002.

LaRoche, J., and Breitbarth, E.: Importance of the diazotrophs as a source of new nitrogen in the ocean, Journal of Sea Research, 53, 67-91, 2005.

Lawson, S. J., Keywood, M. D., Galbally, I. E., Gras, J. L., Cainey, J. M., Cope, M. E., Krummel, P. B., Fraser, P. J., Steele, L. P., Bentley, S. T., Meyer, C. P., Ristovski, Z., and Goldstein, A. H.: Biomass burning emissions of trace gases and particles in marine air at Cape Grim, Tasmania, Atmospheric Chemistry and Physics, 15, 13393-13411, 2015.

Lim, Y., Tan, Y., Perri, M., Seitzinger, S., and Turpin, B.: Aqueous chemistry and its role in secondary organic aerosol (SOA) formation, Atmospheric Chemistry and Physics, 10, 10521-10539, 2010.

Lin, C.-J., and Pehkonen, S. O.: The chemistry of atmospheric mercury: a review, Atmospheric Environment, 33, 2067-2079, 1999.

Liousse, C., Devaux, C., Dulac, F., and Cachier, H.: Aging of savanna biomass burning aerosols: Consequences on their optical properties, Journal of Atmospheric Chemistry, 22, 1-17, 1995.

Lobert, J. M., Keene, W. C., Logan, J. A., and Yevich, R.: Global chlorine emissions from biomass burning: Reactive chlorine emissions inventory, Journal of Geophysical Research: Atmospheres, 104, 8373-8389, 1999.

Locatelli, R., Bousquet, P., Hourdin, F., Saunois, M., Cozic, A., Couvreux, F., Grandpeix, J. Y., Lefebvre, M. P., Rio, C., Bergamaschi, P., Chambers, S. D., Karstens, U., Kazan, V., van der Laan, S., Meijer, H. A. J., Moncrieff, J., Ramonet, M., Scheeren, H. A., Schlosser, C., Schmidt, M., Vermeulen, A., and Williams, A. G.: Atmospheric transport and chemistry of trace gases in LMDz5B: evaluation and implications for inverse modelling, Geoscientific Model Development, 8, 129-150, 2015.

Luo, C., Mahowald, N., Bond, T., Chuang, P., Artaxo, P., Siefert, R., Chen, Y., and Schauer, J.: Combustion iron distribution and deposition, Global Biogeochemical Cycles, 22, 2008.

Mallet, M. D., Cravigan, L. T., Milic, A., Alroe, J., Ward, J., Keywood, M. D., Ristovski, Z. D., Williams, L. R., Selleck, P., and Miljevic, B.: Composition, size and cloud condensation nuclei activity of smoke from north Australian savannah fires, Atmospheric Chemistry and Physics, 2016, submitted.

Manninen, H. E., Petaja, T., Asmi, E., Riipinen, I., Nieminen, T., Mikkila, J., Horrak, U., Mirme, A., Mirme, S., Laakso, L., Kerminen, V. M., and Kulmala, M.: Long-term field measurements of charged and neutral clusters using Neutral cluster and Air Ion Spectrometer (NAIS), Boreal Environment Research, 14, 591-605, 2009.

McFiggans, G., Artaxo, P., Baltensperger, U., Coe, H., Facchini, M. C., Feingold, G., Fuzzi, S., Gysel, M., Laaksonen, A., Lohmann, U., Mentel, T. F., Murphy, D. M., O'Dowd, C. D., Snider, J. R., and Weingartner, E.: The effect of physical and chemical aerosol properties on warm cloud droplet activation, Atmospheric Chemistry and Physics, 6, 2593-2649, 2006.

Melendez-Perez, J. J., Fostier, A. H., Carvalho, J. A., Windmöller, C. C., Santos, J. C., and Carpi, A.: Soil and biomass mercury emissions during a prescribed fire in the Amazonian rain forest, Atmospheric Environment, 96, 415-422, 2014.

Meyer, C., Cook, G., Reisen, F., Smith, T., Tattaris, M., Russell-Smith, J., Maier, S., Yates, C., and Wooster, M.: Direct measurements of the seasonality of emission factors from savanna fires in northern Australia, Journal of Geophysical Research: Atmospheres (1984–2012), 117, 2012.

Meyer, C. P., Luhar, A. K., and Mitchell, R. M.: Biomass burning emissions over northern Australia constrained by aerosol measurements: I—Modelling the distribution of hourly emissions, Atmospheric Environment, 42, 1629-1646, 2008.

Milic, A., Mallet, M. D., Cravigan, L. T., Alroe, J., Ristovski, Z. D., Selleck, P., Lawson, S. J., Ward, J., Desservettaz, M. J., Paton-Walsh, C., Williams, L. R., Keywood, M. D., and Miljevic, B.: Aging of aerosols emitted from biomass burning in northern Australia, Atmospheric Chemistry and Physics Discussions, 2016, 1-24, 10.5194/acp-2016-730, 2016.

Mirme, A., Tamm, E., Mordas, G., Vana, M., Uin, J., Mirme, S., Bernotas, T., Laakso, L., Hirsikko, A., and Kulmala, M.: A wide-range multi-channel Air Ion Spectrometer, Boreal Environmental Research, 12, 247-264, 2007.

Mochida, M., and Kawamura, K.: Hygroscopic properties of levoglucosan and related organic compounds characteristic to biomass burning aerosol particles, Journal of Geophysical Research: Atmospheres (1984–2012), 109, 2004.

National-Environment-Protection-Council-Service-Corporation: National Environment Protection (Air Toxics) Measure, 2011.

Novakov, T., and Corrigan, C.: Cloud condensation nucleus activity of the organic component of biomass smoke particles, Geophysical Research Letters, 23, 2141-2144, 1996.

Packham, D., Tapper, N., Griepsma, D., Friedli, H., Hellings, J., and Harris, S.: Release of Mercury from Biomatter after Burning: A Preliminary Investigation of Biomatter and Soils, Air Quality and Climate Change, 24-27, 2009.

Paris, R., Desboeufs, K., Formenti, P., Nava, S., and Chou, C.: Chemical characterisation of iron in dust and biomass burning aerosols during AMMA-SOP0/DABEX: implication for iron solubility, Atmospheric Chemistry and Physics, 10, 4273-4282, 2010.

Penner, J., Chuang, C., and Grant, K.: Climate forcing by carbonaceous and sulfate aerosols, Climate Dynamics, 14, 839-851, 1998.

Pirrone, N., Cinnirella, S., Feng, X., Finkelman, R. B., Friedli, H. R., Leaner, J., Mason, R., Mukherjee, A. B., Stracher, G. B., Streets, D. G., and Telmer, K.: Global mercury emissions to the atmosphere from anthropogenic and natural sources, Atmospheric Chemistry and Physics, 10, 5951-5964, 2010.

Radhi, M., Box, M. A., Box, G. P., and Mitchell, R. M.: Biomass-burning aerosol over northern Australia, Australian Meteorological and Oceanographic Journal, 62, 25, 2012.

Rea, A. W., Lindberg, S. E., Scherbatskoy, T., and Keeler, G. J.: Mercury accumulation in foliage over time in two northern mixed-hardwood forests, Water, Air, and Soil Pollution, 133(1-4), 49-67, 2002.

Reid, J. S., Hobbs, P. V., Ferek, R. J., Blake, D. R., Martins, J. V., Dunlap, M. R., and Liousse, C.: Physical, chemical, and optical properties of regional hazes dominated by smoke in Brazil, Journal of Geophysical Research: Atmospheres (1984–2012), 103, 32059-32080, 1998.

Rosen, J., Young, S., Laby, J., Kjome, N., and Gras, J.: Springtime aerosol layers in the free troposphere over Australia: Mildura Aerosol Tropospheric Experiment (MATE 98), Journal of Geophysical Research: Atmospheres (1984–2012), 105, 17833-17842, 2000.

Rubin, M., Berman-Frank, I., and Shaked, Y.: Dust-and mineral-iron utilization by the marine dinitrogen-fixer Trichodesmium, Nature Geoscience, 4, 529-534, 2011.

Russell-Smith, J., Yates, C. P., Whitehead, P. J., Smith, R., Craig, R., Allan, G. E., Thackway, R., Frakes, I., Cridland, S., Meyer, M. C. P., and Gill, M.: Bushfires' down under': patterns and implications of contemporary Australian landscape burning, International Journal of Wildland Fire, 16, 361-377, 2007.

Russell-Smith, J., Cook, G. D., Cooke, P. M., Edwards, A. C., Lendrum, M., Meyer, C., and Whitehead, P. J.: Managing fire regimes in north Australian savannas: applying Aboriginal approaches to contemporary global problems, Frontiers in Ecology and the Environment, 11, e55-e63, 2013.

Schroth, A. W., Crusius, J., Sholkovitz, E. R., and Bostick, B. C.: Iron solubility driven by speciation in dust sources to the ocean, Nature Geoscience, 2, 337-340, 2009.

Sedwick, P. N., Sholkovitz, E. R., and Church, T. M.: Impact of anthropogenic combustion emissions on the fractional solubility of aerosol iron: Evidence from the Sargasso Sea, Geochemistry, Geophysics, Geosystems, 8, 2007.

Shen, H., Huang, Y., Wang, R., Zhu, D., Li, W., Shen, G., Wang, B., Zhang, Y., Chen, Y., Lu, Y., Chen, H., Li, T., Sun, K., Li, B., Liu, W., Liu, J., and Tao, S.: Global Atmospheric Emissions of Polycyclic Aromatic Hydrocarbons from 1960 to 2008 and Future Predictions, Environmental Science & Technology, 47, 6415-6424, 10.1021/es400857z, 2013.

Shi, Y., Matsunaga, T., Saito, M., Yamaguchi, Y., and Chen, X.: Comparison of global inventories of CO_2 emissions from biomass burning during 2002–2011 derived from multiple satellite products, Environmental Pollution, 206, 479-487, 2015.

Sinreich, R., Friess, U., Wagner, T., and Platt, U.: Multi axis differential optical absorption spectroscopy (MAX-DOAS) of gas and aerosol distributions, Faraday Discuss, 130, 153-164, 2005.

Sprovieri, F., Pirrone, N., Bencardino, M., D'Amore, F., Carbone, F., Cinnirella, S., Mannarino, V., Landis, M., Ebinghaus, R., Weigelt, A., Brunke, E. G., Labuschagne, C., Martin, L., Munthe, J., Wängberg, I., Artaxo, P., Morais, F., Cairns, W., Barbante, C., Diéguez, M. D. C., Garcia, P. E., Dommergue, A., Angot, H., Magand, O., Skov, H., Horvat, M., Kotnik, J., Read, K. A., Neves, L. M., Gawlik, B. M., Sena, F., Mashyanov, N., Obolkin, V. A., Wip, D., Feng, X. B., Zhang, H., Fu, X., Ramachandran, R., Cossa, D., Knoery, J., Marusczak, N., Nerentorp, M., and Norstrom, C.: Atmospheric Mercury Concentrations observed at ground-based monitoring sites globally distributed in the framework of the GMOS network, Atmospheric Chemistry and Physics Discussions, 2016, 1-32, 2016.

Steffen, A., Douglas, T., Amyot, M., Ariya, P., Aspmo, K., Berg, T., Bottenheim, J., Brooks, S., Cobbett, F., Dastoor, A., Dommergue, A., Ebinghaus, R., Ferrari, C., Gardfeldt, K., Goodsite, M. E., Lean, D., Poulain, A. J., Scherz, C., Skov, H., Sommar, J., and Temme, C.: A synthesis of atmospheric mercury depletion event chemistry in the atmosphere and snow, Atmospheric Chemistry and Physics, 8, 1445-1482, 2008.

Stokes, R., and Robinson, R.: Interactions in aqueous nonelectrolyte solutions. I. Solute-solvent equilibria, The Journal of Physical Chemistry, 70, 2126-2131, 1966.

Tuch, T. M., Haudek, A., Müller, T., Nowak, A., Wex, H., and Wiedensohler, A.: Design and performance of an automatic regenerating adsorption aerosol dryer for continuous operation at monitoring sites, Atmos. Meas. Tech., 2, 417-422, 2009.

Twomey, S.: Aerosols, clouds and radiation, Atmospheric Environment. Part A. General Topics, 25, 2435-2442, 1991.

van der Werf, G. R., Randerson, J. T., Giglio, L., Collatz, G., Mu, M., Kasibhatla, P. S., Morton, D. C., DeFries, R., Jin, Y. v., and van Leeuwen, T. T.: Global fire emissions and the contribution of deforestation, savanna, forest, agricultural, and peat fires (1997–2009), Atmospheric Chemistry and Physics, 10, 11707-11735, 2010.

Wang, X., Thai, P. K., Li, Y., Li, Q., Wainwright, D., Hawker, D. W., and Mueller, J. F.: Changes in atmospheric concentrations of polycyclic aromatic hydrocarbons and polychlorinated biphenyls between the 1990s and 2010s in an Australian city and the role of bushfires as a source, Environmental Pollution, 213, 223-231, 2016.

Wang, X., P.K., T., Mallet, M. D., Desservettaz, M. J., Hawker, D. W., Keywood, M. K., Miljevic, B., Paton-Walsh, C., Gallen, M., and Mueller, J. F.: Emissions of selected semivolatile organic chemicals from forest and savannah fires, Environmental Science & Technology, 2016, under review.

Whittlestone, S., and Zahorowski, W.: Baseline radon detectors for shipboard use: Development and deployment in the First Aerosol Characterization Experiment (ACE 1), Journal of Geophysical Research: Atmospheres, 103, 16743-16751, 1998.

Wigder, N., Jaffe, D., and Saketa, F.: Ozone and particulate matter enhancements from regional wildfires observed at Mount Bachelor during 2004–2011, Atmospheric Environment, 75, 24-31, 2013.

Williams, A. G., Chambers, S., Zahorowski, W., Crawford, J., Matsumoto, K., and Uematsu, M.: Estimating the Asian radon flux density and its latitudinal gradient in winter using ground-based radon observations at Sado Island, Tellus B, 61, 732-746, 2009.

Williams, A. G., Zahorowski, W., Chambers, S., Griffiths, A., Hacker, J. M., Element, A., and Werczynski, S.: The vertical distribution of radon in clear and cloudy daytime terrestrial boundary layers, Journal of the Atmospheric Sciences, 68, 155-174, 2011.

Winton, V., Bowie, A., Edwards, R., Keywood, M., Townsend, A., van der Merwe, P., and Bollhöfer, A.: Fractional iron solubility of atmospheric iron inputs to the Southern Ocean, Marine Chemistry, 177, 20-32, 2015.

Winton, V., Edwards, R., Bowie, A., Keywood, M., Williams, A., Chambers, S., Selleck, P., Desservettaz, M., Mallet, M., and Paton-Walsh, C.: Dry season aerosol iron solubility in tropical northern Australia, Atmospheric Chemistry and Physics Discussions, doi:10.5194/acp-2016-419, 2016.

Wong, J., and Li, Z.: Retrieval of optical depth for heavy smoke aerosol plumes: uncertainties and sensitivities to the optical properties, Journal of the Atmospheric Sciences, 59, 250-261, 2002.

Yokelson, R. J., Crounse, J. D., DeCarlo, P. F., Karl, T., Urbanski, S., Atlas, E., Campos, T., Shinozuka, Y., Kapustin, V., Clarke, A. D., Weinheimer, A., Knapp, D. J., Montzka, D. D., Holloway, J., Weibring, P., Flocke, F., Zheng, W., Toohey, D., Wennberg, P. O., Wiedinmyer, C., Mauldin, L., Fried, A., Richter, D., Walega, J., Jimenez, J. L., Adachi, K., Buseck, P. R., Hall, S. R., and Shetter, R.: Emissions from biomass burning in the Yucatan, Atmospheric Chemistry and Physics, 9, 5785-5812, 2009.